ISSN 0280-5316
ISRN LUTFD2/TFRT--5852--SE

# Agility enhancement and tyre estimation for automotive vehicles

Ola Waldemarsson

Department of Automatic Control
Lund University
March 2010

**Lund University**
**Department of Automatic Control**
**Box 118**
**SE-221 00 Lund Sweden**

*Document name*
MASTER THESIS

*Date of issue*
March 2010

*Document Number*
ISRN LUTFD2/TFRT--5852--SE

*Author(s)*
Ola Waldemarsson

*Supervisor*
Jens Kalkkuhl Daimler AG, Germany
Karl-Erik Årzén Automatic Control, Lund (Examiner)

*Sponsoring organization*

*Title and subtitle*
Agility enhancement and tyre estimation for automotive vehicles (Förbättrad manövrerbarhet och skattning av däcksegenskaper för fordon)

*Abstract*
Every car has its own cornering dynamics, some are oversteered, meaning that they respond more to a steering input, and some are understeered, responding less to a steering input. These dynamics depend on a wide range of parameters, the size and weight of a car and the distribution of the weight to name a few. The main part of this thesis is aimed at controlling the cornering dynamics. More specifically, this thesis deals with increase or decrease the oversteering of a Mercedes car, depending on the situation. This will be achieved by shifting the wheel loads using the Active Body Control, or ABC, of a Mercedes S-class car. During normal driving, an open-loop control scheme will increase the oversteering. As this control scheme will push the car to its limits during cornering, the car might lose control. As the car loses control, the control scheme will shift from increasing the oversteering to decreasing it. When the controller identifies a loss of control, it will shift from the open-loop control scheme to a closed-loop sliding mode controller working to decrease the oversteering. The two controllers require some data which is not measurable. Therefore an observer was used to observe the non-measurable states. The observer used contains a tyre model to be able to calculate the different forces acting on the car. This tyre model contains a parameter set describing the tyres. The last part of this thesis describes a way to choose this parameter set more precisely with least squares estimation of the longitudinal tyre stiffness. This stiffness varies between summer and winter tyres and the estimation of this parameter enables the observer to use different parameter sets for winter and summer tyres.

*Keywords*

*Classification system and/or index terms (if any)*

*Supplementary bibliographical information*

*ISSN and key title*
0280-5316

*ISBN*

*Language*
English

*Number of pages*
50

*Recipient's notes*

*Security classification*

# Acknowledgements

I would like to give thanks to the vehicle dynamics team in the GR/EAV department in research and development at the Mercedes facilities in Sindelfingen, Germany. Especially I would like to thank Prof. Dr. Jens Kalkkuhl for his supervision and support for this thesis. I would also like to thank Prof. Karl-Erik Årzén for his supervision from Lunds University and for giving me this opportunity.

# Notation

Bold letters denotes vectors.

### Indices

| | |
|---|---|
| CoG | Centre of Gravity |
| D | setpoint |
| f | front |
| i | wheel index, 1, 2, 3 or 4 |
| j | axle index, f or r |
| r | rear |
| x | longitudinal direction |
| y | lateral direction |
| z | vertical direction |

### Symbols

| | |
|---|---|
| $\alpha$ | wheel slip angle |
| $\beta$ | sideslip angle |
| $\gamma$ | roll moment distribution |
| $\delta$ | steering wheel angle |
| $\mu$ | road-tyre friction |
| $\omega$ | rotational speed |
| $\varphi$ | roll angle |
| $\theta$ | pitch angle |
| $\psi$ | yaw angle |
| | |
| a | acceleration |
| C | longitudinal tyre stiffness |
| F | force |
| h | height |
| J | Torque |
| $l_j$ | distance from centre of gravity to axle *j* |
| L | wheel base |
| m | mass |
| $r_{Dyn}$ | Dynamic wheel radius |
| s | track width |
| v | speed |

# Contents

# 1. Introduction

Electronic systems in cars increase the safety and effectiveness of the car through electronics and software rather than through mechanics or hydraulics. An example of these systems is the Engine Control Unit which controls the fuel injections, spark timing, etc. increasing the engine efficiency through calculations in an onboard computer. The amount of electronic applications such as this is rapidly increasing and has done so the last decades. Estimates imply that 80% of new innovations in cars now come from electronics.

In the area of electronic systems, the car industry is particularly interested in active safety systems and driver assistance. While passive safety systems aim at decreasing the risk of personal injury in a crash, active safety systems aim at avoiding crashes altogether. The area of active safety systems has seen many new innovations the last years, such as Electronic Stability Program, side wind compensation and Adaptive Cruise Control.

These controllers utilize different actuators controllable with electronic signals as well as mechanics. The ESP for instance uses the individual wheel brakes and the Adaptive Cruise Control works through the Engine Control Unit. The side wind compensation can be actuated by slightly turning the vehicle's steering wheels to compensate or by using Active Body Control. Active Body Control is a system which uses the cars suspension to distribute the wheel load which in turn changes the dynamics of the vehicle.

Information on Electronic Stability Program, Side Wind Compensation and Adaptive Cruise Control can be found in [1], [2] and [3] respectively. Information on ABC can be found in [4].

## 1.1 Goals and motivation

The following points are the goals of this master thesis:

- Increase the agility of a turning Mercedes car using Active Body Control.

  A Mercedes car in the S-class is an under steered car. With Active Body Control, or ABC, it is possible to enhance the agility of the car, increasing the yaw rate while turning. While this reduces the stability, and therefore the safety of the car, it will increase the driving experience to make the car more entertaining.

- Limit the sideslip angle to a set value.

  To increase the safety of a car driving with enhanced agility, a limiter of the sideslip angle can be used. The sideslip angle is the angle between the car velocity and the longitudinal component. This limiter would catch the car as it starts to slide, or at least reduce the rate of loss of control, and so increase the safety.

- Implement an online estimator of certain tyre parameters to estimate if summer or winter tyres are used

In an observer of, for instance, the tyre forces, a model of the tyres is needed. This model has a set of parameters whose accuracy affects the result of the estimation. With unknown tyres this parameter set needs to be more general. If the type of tyres is known, a more precise parameter set can be chosen and so improve the estimation.

## 1.2 Tools

The controllers and the estimator presented in this project have been made in Matlab and Simulink with some minor parts written in C#.

The controllers have mostly been tested with a car simulation tool known as CASCaDE. This is a simulation tool used in the Simulink environment which is written mostly in C# and is developed by Daimler. It contains detailed models of different Mercedes cars. The controllers have also been tested in a test vehicle equipped with Active Body Control. The simulations with CASCaDE were made with a model of the test vehicle used.

The estimator has been tested with measurements from two different test vehicles. It has also been tested in real time. These tests, as well as the tests of the controllers, were carried out at the test track at the Mercedes facilities in Sindelfingen, Germany. Personnel from the GR/EAV department at the Mercedes facilities in Sindelfingen were test drivers.

# 2. Model

The car is modelled as a four wheel model, as opposed to the simpler single track model often used. This choice is necessary since the model has to be able to distinguish between the behaviour of the left and right wheels. The actuator used, Active Body Control, redistributes the wheel loads to change the agility of the car, and an accurate analysis of this with a single track model is not possible.

## 2.1 Four wheel model

A turning vehicle with tyre forces is shown in Figure 1. The lateral components of the wheel forces must add up to the force $m \cdot a_y$, where $a_y$ is the lateral acceleration. The same holds for the torque from the wheel forces on the centre of gravity, they must correspond to the torque $J_\Psi \cdot \ddot{\Psi}$, where $\ddot{\Psi}$ is the rotational acceleration around the centre of gravity.

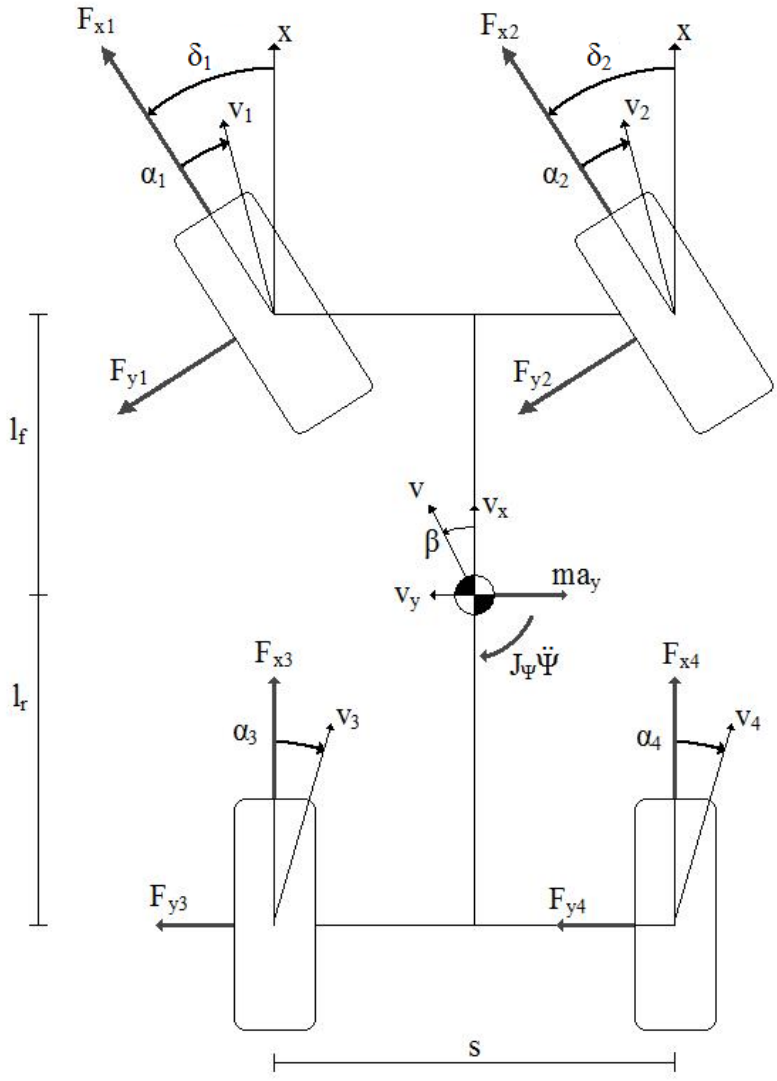


Figure 1. Four wheel model of the car

Notable distances in the model are the distances from the front and rear axes to the centre of gravity which are denoted $l_f$ and $l_r$ respectively. The track width is denoted s. Notable angles are the wheel angles, $\delta_i$, and the wheel slip angles, $\alpha_i$. The wheel speeds are denoted by $v_i$, and the car lateral and longitudinal speed, $v_y$ and $v_x$. The angle between the car speed, v, and its longitudinal component is the sideslip angle, $\beta$.

With a force and a torque balance, expressions for the lateral acceleration and the yaw acceleration, respectively, are derived. The expressions are:

$$m \cdot a_y = \sum_{i=1}^{4} \cos(\delta_i) \cdot F_{yi} + \sum_{i=1}^{4} \sin(\delta_i) \cdot F_{xi}$$

$$J_\Psi \cdot \ddot{\Psi} = a_1 \cdot F_{y1} + a_2 \cdot F_{y2} - a_3 \cdot F_{y3} - a_4 \cdot F_{y4} - b_1 \cdot F_{x1} + b_2 \cdot F_{x2} - b_3 \cdot F_{x3} + b_4 \cdot F_{x4},$$

where $\delta_3 = \delta_4 = 0$ and $a_i$ and $b_i$ are distances defined in Figure 2 and 3. The expressions for $a_i$ and $b_i$ are:

$$a_1 = l_v \cdot \cos(\delta_1) + \frac{s}{2} \cdot \sin(\delta_1)$$

$$b_1 = \frac{s}{2} \cdot \cos(\delta_1) - l_v \cdot \sin(\delta_1)$$

$$a_2 = l_v \cdot \cos(\delta_2) - \frac{s}{2} \cdot \sin(\delta_2)$$

$$b_2 = \frac{s}{2} \cdot \cos(\delta_2) + l_v \cdot \sin(\delta_2)$$

$$a_3 = a_4 = l_h,\ b_3 = b_4 = \frac{s}{2}$$

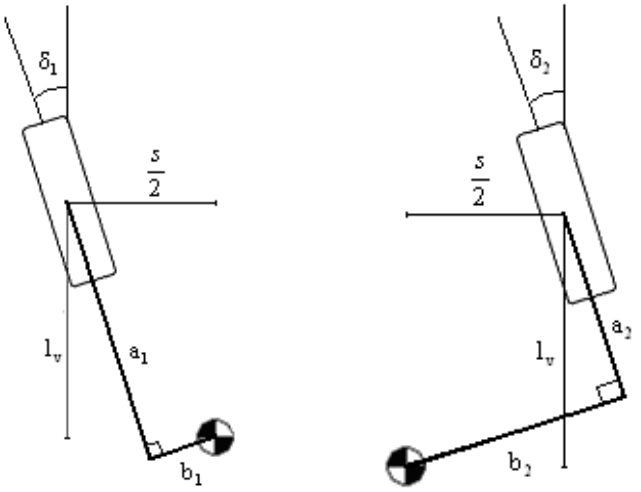


Figure 2 and 3. Distances from the front wheels to the centre of gravity

Since the control input affects the load distribution, it is necessary to extend this model to include the wheel loads. For this, models of the tyres are needed.

## 2.2 Tyre model

Several different tyre models are available. The simplest is a linear relation between the wheel forces and the slip, which is only valid for smaller values on the angles and velocities. In this thesis, a more detailed model is used for two reasons. The model will be used to derive a sideslip limiter and when such a limiter is needed the tyres are acting outside of their linear range. Secondly, the tyre model needs to model the wheel forces dependency on the wheel load. A model from [5] is chosen.

The slip of a wheel is the normalized difference between the car reference speed and the wheel speed. Zero means that the wheel is free rolling, without a torque from the engine, and 1.00 means that the wheel is spinning, without grip when the car stands still. The longitudinal, $\lambda_x$, and lateral, $\lambda_y$, slip are calculated as

$$\lambda_{xi} = \frac{\omega_i \cdot r_{dyn} - v_x}{\max\left(\omega_i \cdot r_{dyn}, v_x\right)}$$

$$\lambda_{yi} = \sin\left(\alpha_i\right)$$

$$\text{and } \lambda_{Ri} = \sqrt{\lambda_{xi}^2 + \lambda_{yi}^2}$$

In these equations $\omega_i$ is the angular speed of wheel i and $r_{dyn}$ is the dynamic wheel radius. $v_x$ is the speed of the centre of gravity of the car and $\alpha_i$ is the wheel slip angle.

Due to changes in tyre pressure and wheel loads, the tyre deflection changes with time. This means that the effective wheel radius, the dynamic wheel radius, will be unknown and time varying, although with small variations.

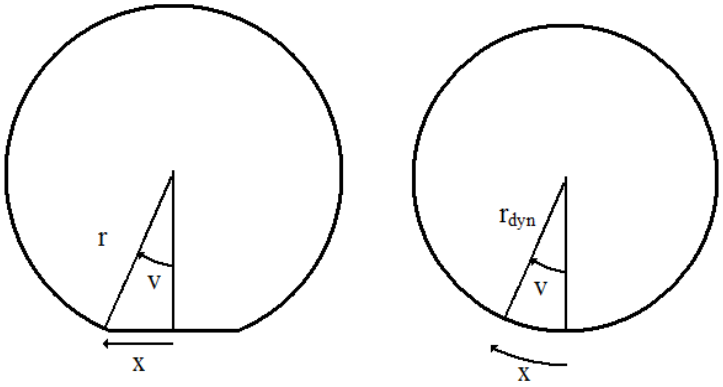


Figure 4. The dynamic wheel radius

The slips are used in the tyre model in the expressions for the longitudinal and lateral wheel forces:

$$F_{xi} = \begin{cases} \dfrac{C_{xi}\lambda_{xi}}{\left(\xi_{xi} - 1\right)^2 + C_{xi}^*\xi_{xi}} & \xi_{xi} \le 1 \\ \dfrac{\lambda_{xi}}{\lambda_{Ri}}\mu_{xi}F_{zi} & \xi_{xi} > 1 \end{cases}$$

$$\xi_{xi} = \frac{\lambda_{Ri}}{\lambda_{x\max}}, \quad \lambda_{x\max} = \lambda_{x0} \cdot \mu_H, \qquad C_{xi} = C_{x0} \cdot \frac{F_{zi}}{F_N}$$

$$C_{xi}^* = \frac{\lambda_{x0}}{\mu_{x0} + \mu_{x1} F_{zi}} \cdot \frac{C_{xi}}{F_{zi}}, \qquad \mu_{xi} = (\mu_{x0} + \mu_{x1} F_{zi}) \mu_H, \qquad \lambda_{Ri} = \sqrt{\lambda_{xi}^2 + \lambda_{yi}^2},$$

where $\lambda_{x0}$, $\mu_H$, $\mu_{x0}$, $\mu_{x1}$ and $C_{x0}$ are all tyre parameters. For the lateral wheel forces the following expressions are used:

$$F_{yi} = \begin{cases} \dfrac{C_{yi} \lambda_{yi}}{(\xi_{yi} - 1)^2 + C_{yi}^* \xi_{yi}} & \xi_{yi} \le 1 \\ \dfrac{\lambda_{yi}}{\lambda_{Ri}} \mu_{yi} F_{zi} & \xi_{yi} > 1 \end{cases}$$

$$\xi_{yi} = \frac{\lambda_{Ri}}{\lambda_{y\max}}, \quad \lambda_{y\max} = (\lambda_{y0} + \lambda_{y1} F_{zi}) \mu_H, \quad C_{yi} = 2 C_{y0} \frac{F_{zi} F_N}{F_N^2 + F_{zi}^2}$$

$$C_{yi}^* = \frac{\lambda_{y0} + \lambda_{y1} F_{zi}}{\mu_{y0} + \mu_{y1} F_{zi}} \cdot \frac{C_{yi}}{F_{zi}}, \qquad \mu_{yi} = (\mu_{y0} + \mu_{y1} F_{zi}) \mu_H,$$

where $\lambda_{y0}$, $\lambda_{y1}$, $\mu_H$, $\mu_{y0}$, $\mu_{y1}$ and $C_{y0}$ are tyre parameters. In this wheel model the longitudinal and lateral forces depend on the wheel loads.

## 2.3 Wheel loads

The actuator that will be used for the sideslip limiter is the Active Body Control or ABC. The suspension redistributes the mass of the car diagonally over the wheels. This means that the loads on the front left and rear right wheels, for example, are reduced and the loads on the front right and rear left are increased. Because of this the actuator only has one input, the roll moment distribution, γ.

The dynamics of the wheel loads are:

$$F_{1z} = F_{N,f} - \frac{l_r}{L} \cdot \frac{1}{s} \left( d_{roll} \cdot \dot{\varphi} + c_{roll,f} \cdot \varphi + m \cdot a_y \cdot h_{CoR} \right) - \left( \kappa_{0,s} + \Delta\kappa_s \right) \cdot \frac{c_s \cdot \varphi}{s} + \Delta F_{ABC,1}$$

$$F_{2z} = F_{N,f} + \frac{l_r}{L} \cdot \frac{1}{s} \left( d_{roll} \cdot \dot{\varphi} + c_{roll,f} \cdot \varphi + m \cdot a_y \cdot h_{CoR} \right) + \left( \kappa_{0,s} + \Delta\kappa_s \right) \cdot \frac{c_s \cdot \varphi}{s} + \Delta F_{ABC,2}$$

$$F_{3z} = F_{N,r} - \frac{l_f}{L} \cdot \frac{1}{s} \left( d_{roll} \cdot \dot{\varphi} + c_{roll,f} \cdot \varphi + m \cdot a_y \cdot h_{CoR} \right) - \left( 1 - \kappa_{0,s} - \Delta\kappa_s \right) \cdot \frac{c_s \cdot \varphi}{s} + \Delta F_{ABC,3}$$

$$F_{4z} = F_{N,r} + \frac{l_f}{L} \cdot \frac{1}{s} \left( d_{roll} \cdot \dot{\varphi} + c_{roll,f} \cdot \varphi + m \cdot a_y \cdot h_{CoR} \right) + \left( 1 - \kappa_{0,s} - \Delta\kappa_s \right) \cdot \frac{c_s \cdot \varphi}{s} + \Delta F_{ABC,4}$$

In these equations, $F_{N,j}$ is the nominal wheel load of axle j. $\Delta F_{ABC,4}$ is the load wheel term from the active suspension containing the control input that will be

used in the controllers presented in the next two sections. The remaining two terms in the equations above models the effect on the wheel loads from the roll and the pitch of the car.

$$\Delta F_{ABC,1} = \frac{\omega_{ABC}}{4}, \qquad \Delta F_{ABC,2} = -\frac{\omega_{ABC}}{4}$$

$$\Delta F_{ABC,3} = -\frac{\omega_{ABC}}{4}, \qquad \Delta F_{ABC,4} = \frac{\omega_{ABC}}{4}$$

the warp, $\omega_{ABC}$, with unit Newton, is

$$\omega_{ABC} = \frac{4 \cdot m \cdot a_y \cdot h_{CoG}}{s} \cdot \left( \frac{l_r}{L} - \gamma \right).$$

Here the control input, the roll moment distribution, $0 \le \gamma \le 1$, is introduced. The warp will be zero if the distribution is neutral, i.e. if $\gamma = \frac{l_r}{L} \approx 0.5$. A higher value will make the car more understeered and a lower value will make the car more oversteered. The roll moment distribution is signless and therefore only decides the size of the load changes. The sign is decided by the lateral acceleration. Further explanations can be found in [6]

## 2.4 State space formulation

With the relation that $a_y = \dot{v}_y - v_x \dot{\Psi}$, the force and the torque balances in Section 2.1 gives the following state space model describing the car lateral and rotational dynamics. The longitudinal velocity is incorporated in the model as a scheduling variable.

$$\begin{bmatrix} \dot{v}_y \\ \ddot{\Psi} \end{bmatrix} = \begin{bmatrix} 0 & -v_x \\ 0 & 0 \end{bmatrix} \begin{bmatrix} v_y \\ \dot{\Psi} \end{bmatrix} + \begin{bmatrix} \frac{\cos(\delta_1)}{m} & \frac{\cos(\delta_2)}{m} & \frac{1}{m} & \frac{1}{m} \\ \frac{a_1(\delta_1)}{J_\Psi} & \frac{a_2(\delta_2)}{J_\Psi} & -\frac{l_h}{J_\Psi} & -\frac{l_h}{J_\Psi} \end{bmatrix} \begin{bmatrix} F_{y1} \\ F_{y2} \\ F_{y3} \\ F_{y4} \end{bmatrix}$$

$$+ \begin{bmatrix} \frac{\sin(\delta_1)}{m} & \frac{\sin(\delta_2)}{m} & \frac{0}{s} & \frac{0}{s} \\ \frac{b_1(\delta_1)}{J_\Psi} & -\frac{b_2(\delta_2)}{J_\Psi} & -\frac{s}{2 \cdot J_\Psi} & \frac{s}{2 \cdot J_\Psi} \end{bmatrix} \begin{bmatrix} F_{x1} \\ F_{x2} \\ F_{x3} \\ F_{x4} \end{bmatrix}$$

If this expression were to be extended by the tyre and wheel load models presented above, this expression would be highly complex. Roll dynamics would have to be included and four different cases would have to be considered, from $\xi_{xi}$ and $\xi_{yi}$, leading to four different control laws.

Therefore a simplification was made, the wheel forces are now expressed as a nominal force added with a value representing the force change from the roll moment distribution. The nominal forces are the forces given from the presented

wheel model but without the contribution from the ABC, i.e. a Taylor expansion of order 1 is used instead of the complete tyre model.

$$F_{xi} = F_{xi0} + \frac{dF_{xi}}{dF_{zi}} \cdot \Delta F_{zi}(\gamma)$$

$$F_{yi} = F_{yi0} + \frac{dF_{yi}}{dF_{zi}} \cdot \Delta F_{zi}(\gamma)$$

The force from the roll moment distribution, $\Delta F_{zi}(\gamma)$, was defined earlier under wheel loads. The two derivatives are the derivatives of the wheel forces defined in the tyre model with respect to the wheel loads. The nominal forces and their derivatives are all observed with an observer described in [5].

A comparison between the presented four wheel model with the wheel model and the CASCaDE model is presented in Figure 5 and 6 below. The scenario used is a rather hard sinusoidal turn with an amplitude of 80 degree for the steering wheel angle and a peak sideslip angle of 4 degrees. This is well outside the linear range of the tyres.

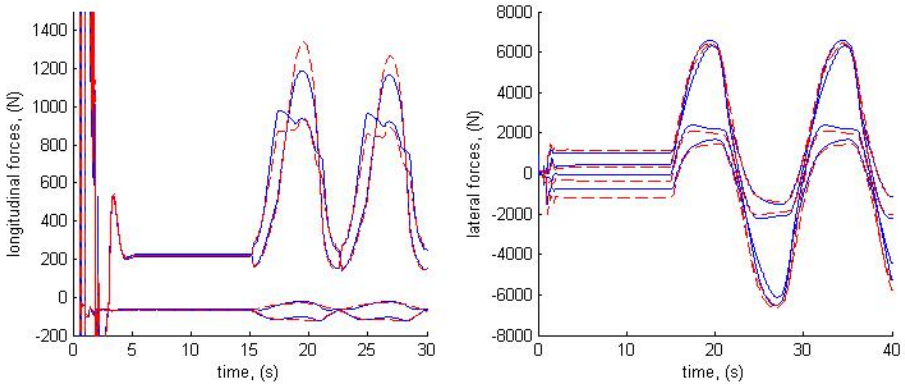


Figure 5. The longitudinal forces (left) and the lateral forces (right) from a sinusoidal turn. The values from the four wheel model (blue solid) are compared to the simulated values from CASCaDE (red dashed)

The large transition in the beginning of the simulation is a result of the initial states in the CASCaDE model. The model corresponds well to the CASCaDE model at high sideslips angles. However, for sideslip angles less than two degrees, the model error increases but during those sideslip angles the sideslip limiter will not be active

Since the comparison is made between the derived model and another, albeit more detailed, model, and not to a real car, an unknown model error might still exist. Therefore a robust controller should be used to limit the sideslip angle.

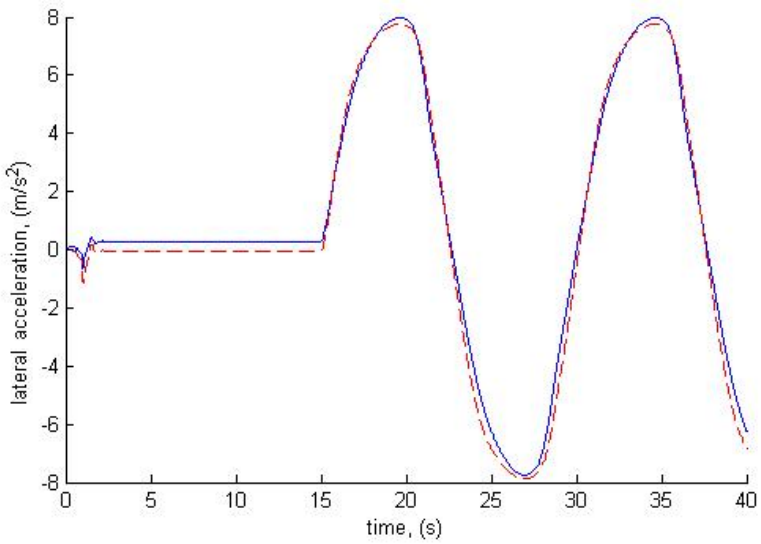


Figure 6. The lateral acceleration. The values from the four wheel model (blue solid) are compared to the simulated values from CASCaDE (red dashed)

# 3. Agility enhancer

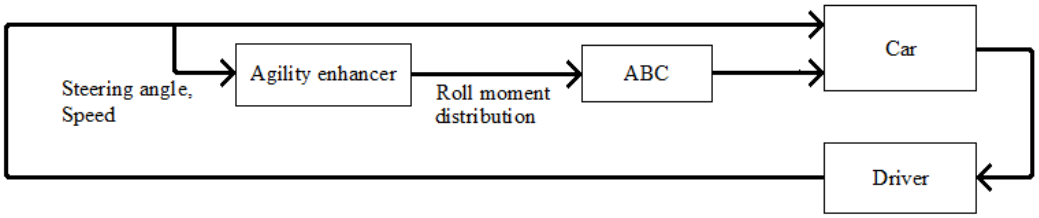


Figure 7. A block diagram over a car with the agility enhancer. The enhancer inputs are the steering and speed signal from the driver and the output is the roll moment distribution

The agility enhancer is a feedforward controller increasing the oversteering of the car. It is a function of the car speed and steering angle and outputs the roll moment distribution. As mentioned above a lower value on γ means a more oversteered car.

The feedforward was derived through simulations with CASCaDE. In simulations the lowest possible roll moment distribution without the car loosing control was found for several speed and steering angle combinations. These values where then used to make a bicubic interpolation of the lowest γ possible for different speed and steering angle combinations up to 120km/h.

For situations when a normal car would loose control, the enhancer would output a stabilizing roll moment distribution. Since the sideslip limiter will be implemented later, this is unwanted. Therefore the enhancer output is limited to values less than $\frac{l_h}{L} \approx 0.5$. Below, the feedforward is shown for a set of different speeds and steering angles.

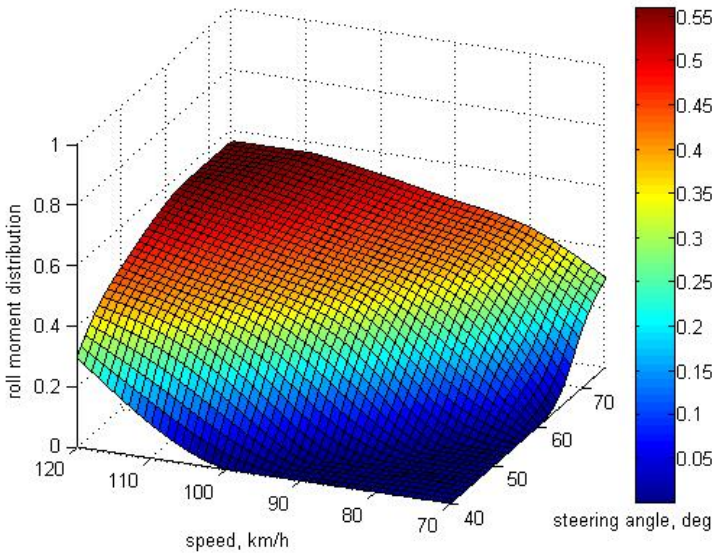


Figure 8. The roll moment distribution

Since the agility enhancer is derived through simulations, it will be zero for all smaller steering angles. In the modeling above it was explained that the distribution is signless and the lateral acceleration will decide the sign of the warp.

If γ is zero for small steering angles and thus for small lateral accelerations, the warp will shift between its two maximums as the lateral acceleration crosses zero.

To prevent this, the distribution is set to neutral, $\gamma = \frac{l_h}{L}$, for small steering angles and a smooth transition between the neutral and the enhancing value is used. The distribution is set to neutral for steering angles less than 10 degrees and the transition from neutral to full activity takes place between 10 and 45 degrees. The same is used for the speed, the enhancer is not active during speeds below 40 km/h and a transition spans from 40 to 45 km/h. The result can be seen in Figure 9.

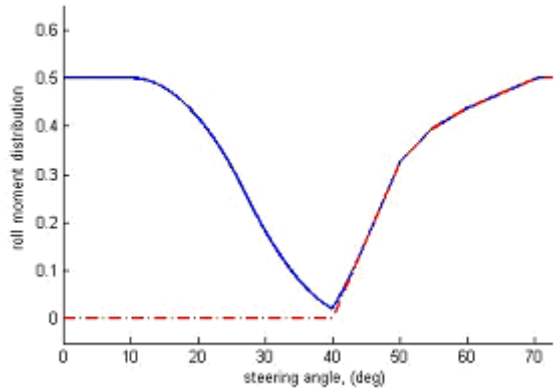


Figure 9. The feedforward signal from the agility enhancer as a function of steering angle. The speed is constant at 100 km/h.

The feedforward controller increases the yaw rate according to Figure 10 below. A higher increase is possible for higher steering angles at lower speeds, such as 80 or 90 km/h. At these speeds the increase can be as much as 70-75 % while for 110 km/h the highest procentual increase is 40 to 45%. The sharp drop in the end of all curves in Figure 10, marks when a car with neutral load distribution would be close to loosing control, i.e. the enhancer output is close to neutral for these steering angles.

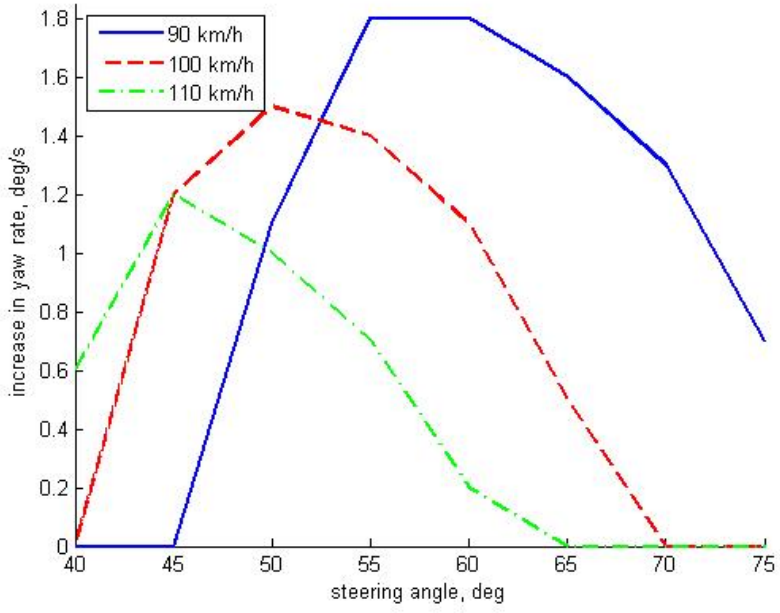


Figure 10. Yaw rate increase for different speeds as a function of the steering angle. The increase is higher for lower speeds around 70 - 90

# 4. Sideslip limiter

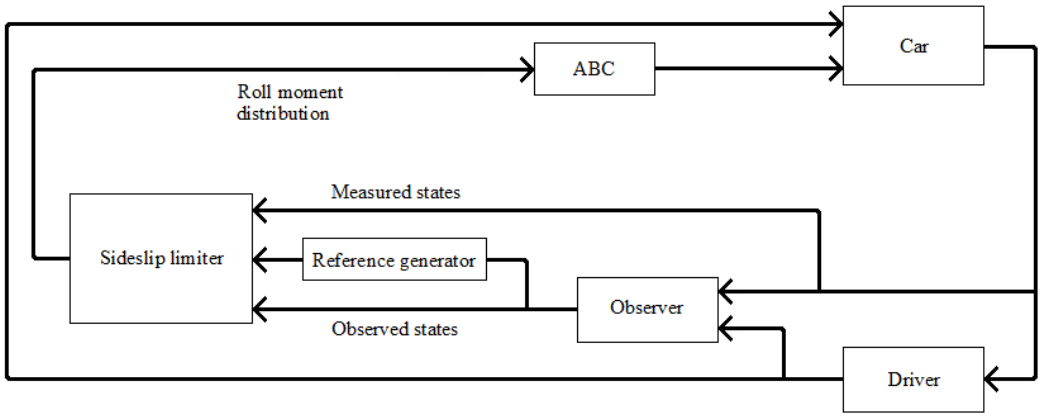


Figure 11. A block diagram of the sideslip limiter with an observer and a reference generator.

Since the agility enhancer is made to push the car to its limits while turning, the car might lose its grip. Therefore some sort of safety system is needed: a controller that recognizes if the car has lost control, disables the agility enhancer and brings the situation back to normal.

This controller will also use the ABC as its actuator and is derived from the model presented before. Since the system is nonlinear and contains uncertainties, a nonlinear and robust control method is chosen.

## 4.1 Sliding mode control

Sliding mode control is a robust control method that turns an n$^{th}$-order single input dynamic system into an equivalent first-order system. This is done by using the tracking errors of the states, $\tilde{x} = \bar{x} - \bar{x}_D$, to create a scalar equation $s(\tilde{x}, t)$, which fulfils the tracking condition when $s(\tilde{x}, t) = 0$. $s(\tilde{x}, t)$ is a weighted sum of the tracking errors.

This scalar equation, $s(\tilde{x}, t) = 0$, defines a surface in the state space, S(t), called the sliding surface and perfect tracking is equivalent to keeping the system at this surface. This turns the surface into an invariant set. The problem can now be solved with a control law that, outside of the sliding surface, fulfils

$$\dot{V} = \frac{d}{dt}\left(\frac{1}{2}s^2\right) \leq -\eta|s|,$$

where $V = \frac{1}{2}s^2$ is a Lyapunov function describing the system and η is a strictly positive constant. This relation means that the Lyapunov function has to be negative definite, i.e. the system trajectories are leading to the sliding surface for all points in the state space outside of the sliding surface. The control law that fulfils this relation will be on the form.

$$u = \hat{b}^{-1} \cdot \left[\hat{u} + K \cdot sign(s)\right]$$

In this control law, $\hat{b}$ would cancel the input dynamics if the dynamics were completely known, and $\hat{u}$ is an estimate of a perfect control that would fulfill

s(**x**,t) = 0. The term $K \cdot sign(s)$ is discontinuous over the sliding surface and its size, K, decides how large uncertainties the controller can overcome. A more thorough description of sliding mode methodology can be found in [8].

## 4.2 Controller

Since the goal of this thesis is to enhance the agility of the car, which is the same as increasing the yaw rate while turning, the yaw rate should not be limited. But since the car might lose control there must be a limit on the sideslip angle and by that, the lateral velocity. Therefore the sliding surface is defined as the error between the sideslip angle and its limit. However, the sideslip limiter will only be active when the sideslip angle is too high. The sliding surface becomes:

$$s = \left(v_y - v_{yD}\right) = 0$$

This sliding surface is a one dimensional surface, i.e. a straight line at $v_y = v_{yD}$ in the state space. This is valid since the sliding mode controller will not be used for tracking but only limiting of one state. Therefore it will only be active during a certain condition, when the lateral velocity error is positive. In the state space plane for the two states of the model, this means that the controller will work to reduce the sideslip angle only when the states are to the right of the sliding surface according to Figure 12.

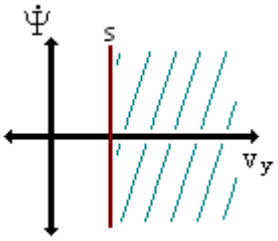


Figure 12. The sliding surface in the state-space plane. s marks the sliding surface at $v_y = v_{yD}$, and the marked area is where the limiter is active.

A Lypunov function is now formed from the scalar quantity s.

$$V = \frac{1}{2}s^2$$

This Lyapunov function has the derivative:

$$\dot{V} = s \cdot \dot{s} = \left(v_y - v_{yD}\right) \cdot \left(\dot{v}_y - \dot{v}_{yD}\right)$$

This function is then expanded with the expressions for $\dot{v}_y$ from the state space formulation together with the simplified wheel forces and the warp. With all this the Lyapunov function is expressed as a function of the control input, i.e., the roll moment distribution.

Solving the equation for the distribution gives:

$$\gamma = \frac{l_h}{L} + \frac{s}{m \cdot a_y \cdot h_{CoG}} \cdot$$

$$\frac{m}{\cos(\delta_1)\frac{dF_{y1}}{dF_{z1}} - \cos(\delta_2)\frac{dF_{y2}}{dF_{z2}} - \frac{dF_{y3}}{dF_{z3}} + \frac{dF_{y4}}{dF_{z4}} + \sin(\delta_1)\frac{dF_{x1}}{dF_{z1}} - \sin(\delta_2)\frac{dF_{x2}}{dF_{z2}}} \cdot$$

$$\left(\frac{1}{m}\cdot\left(\cos(\delta_1)F_{y10} + \cos(\delta_2)F_{y20} + F_{y30} + F_{y40} + \sin(\delta_1)F_{x10} + \sin(\delta_2)F_{x20}\right) - v_x \cdot \dot{\Psi} - \dot{v}_{yD} + K \cdot sign(\tilde{v}_y)\right)$$

with this, the Lyapunov function becomes:

$$\dot{V} = -K\left|\tilde{v}_y\right| \le -\eta \cdot \left|\tilde{v}_y\right|$$

The control law is written on the form $u = \hat{b}^{-1} \cdot \left[\hat{u} - K \cdot sign(s)\right]$ where $\hat{b}$ cancels the input dynamics, û tries to achieve perfect control and $K \cdot sign(s)$ increases the robustness of the controller, i.e. deals with parameter uncertainties and unmodeled dynamics. K is a design parameter for the controller and is based on an estimate of the magnitude of the uncertainties.

In the control signal there are two divisions that need to be considered. First the division $\frac{s}{m \cdot a_y \cdot h_{CoG}}$, where $a_y$ can be zero. This will not be a problem since the controller is deactivated when the lateral acceleration is small. A sideslip angle different from zero implies a lateral acceleration different from zero. The other division includes the derivatives of the wheel loads:

$$\frac{m}{\cos(\delta_1)\frac{dF_{y1}}{dF_{z1}} - \cos(\delta_2)\frac{dF_{y2}}{dF_{z2}} - \frac{dF_{y3}}{dF_{z3}} + \frac{dF_{y4}}{dF_{z4}} + \sin(\delta_1)\frac{dF_{x1}}{dF_{z1}} - \sin(\delta_2)\frac{dF_{x2}}{dF_{z2}}}$$

Simulations in CASCaDE show that the denominator never crosses zero during times when the sideslip limiter is used, but can come very close. Since more noise is expected during a test in a car this denominator will cause problems by crossing zero.

As explained above the sideslip limiter is derived as a tracker but will be used as a limiter. Up to this point it would be possible to use the sliding mode controller to increase the sideslip angle as well but to prevent the possible divisions by zero, parts of the control law will be changed. Instead of the expression in the denominator above, its absolute value will be used which is then limited to values equal to or above a certain limit. This removes the possibility of a zero crossing. With this change the controller will only work as a sideslip limiter.

The limit for the denominator is used as a gain, a tuning parameter that reduces the weight of this term in the control signal. The dynamics that causes the problem arises from the simplification of the wheel forces:

$$F_{xi} = F_{xi0} + \frac{dF_{xi}}{dF_{zi}} \cdot \Delta F_{zi}(\gamma)$$

$$F_{yi} = F_{yi0} + \frac{dF_{yi}}{dF_{zi}} \cdot \Delta F_{zi}(\gamma)$$

To get a value on the control parameter K, the uncertainties in the model of the tyre forces have to be estimated. This was done for steady state turning, comparing the impact of the warp on the longitudinal and lateral forces.

The sideslip limiter has been tested on steady state turning and sinusoidal turning with constant speeds. For these scenarios and with the sideslip limit set to 6 or more, the limiter is not activated until the car has lost control. The controller is able to catch the car as it is losing control, and forces the sideslip angle back to allowed values.

In Figure 13 below the result of a simulation of sinusoidal turning is presented. The turns are made at 120 km/h and the amplitude of the steering input is 75 deg. As explained before the control signal is signless since the warp is calculated with the lateral acceleration. This simulation is made without using the agility enhancer.

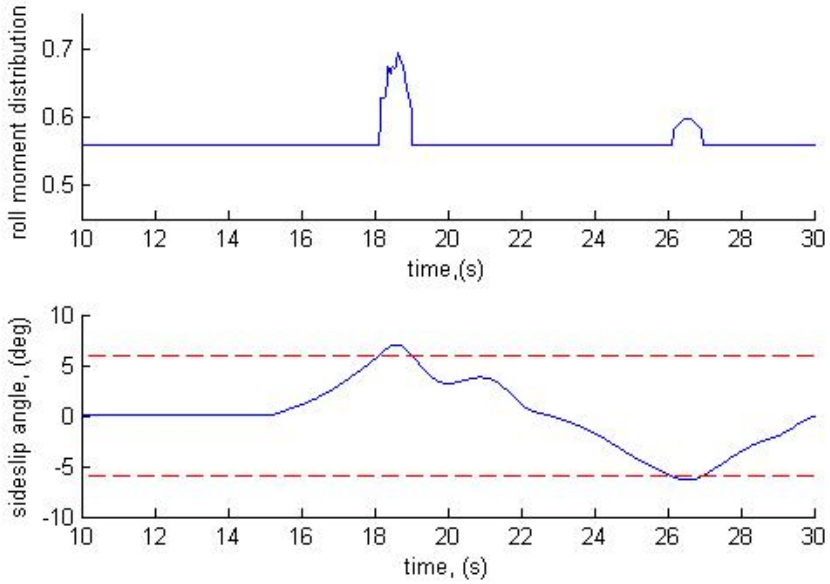


Figure 13. The signal from the sideslip limiter during a sinusoidal turn, (above). The sideslip angle and its limits (below). The sinusoidal turning has an amplitude of 75 deg at a speed of 120 km/h

In a simulation with a normal car, without the sideslip limiter, the car would loose control during the first turn. The limiter reduces the sideslip angle significantly as soon as it crosses its limit. Since the controller is a sliding mode controller it is not activated until the sideslip angle is too large. This means that the sideslip angle will be larger than its limit at some points. This happens after 18 and 16 seconds.

# 5. Implementation & Results

The goal of this thesis is to enhance the agility of a car and to limit the sideslip angle to a set value. Both an enhancer and a limiter have been made and now they will be put together. For this a switch has to be made as well as a reference generator that defines when the system should switch between the two controllers.

Some of the inputs to the controllers are not measurable such as the sideslip angle and the yaw rate. Instead these inputs have to be observed. This is done by software developed at Daimler and described in [5].

In Figure 14 below all the parts of the controller are shown in a block diagram together with the car and driver.

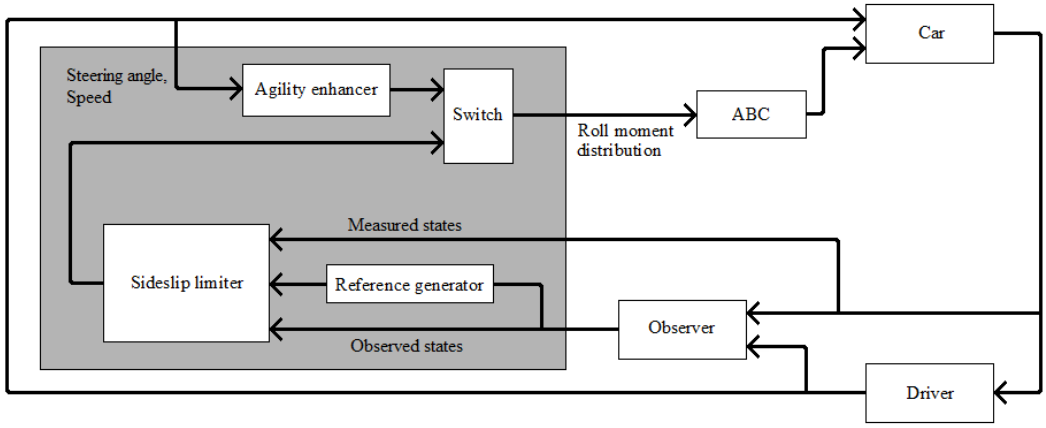


Figure 14. A block diagram of the entire system.

## 5.1 Reference generator

The limit for the controller will be given as a value for the sideslip angle and needs to be transformed to fit the choice of sliding surface. The reference needs to be expressed as lateral velocity and the time derivate of the lateral velocity, $v_y$ and $\dot{v}_y$ respectively, due to the choice of states used in the sliding surface.

A relation between lateral velocity and sideslip angle can easily be derived from Figure 1. The time derivative of that expression will give the second relation needed. An expression which relates the limit on the sideslip angle to a limit on the lateral velocity is:

$$v_{yD} = v_x \cdot \tan(\beta_D)$$

Since the longitudinal velocity is used as a scheduling variable the time derivative becomes:

$$\dot{v}_{yD} = v_x \cdot \frac{1}{\cos^2(\beta_D)} \cdot \dot{\beta}_D$$

Together with the following expression for the time derivative of the side slip angle,

$$\dot{\beta}_D = -a \cdot (\beta_D - \beta)$$

the derivative of the velocity becomes:

$$\dot{v}_{yD} = v_x \cdot \frac{1}{\cos^2(\beta_D)} \cdot \dot{\beta}_D = -v_x \cdot \frac{1}{\cos^2(\beta_D)} \cdot a \cdot (\beta_D - \beta)$$

The expression for the derivative of the sideslip limit, $\dot{\beta}_D = -a \cdot (\beta_D - \beta)$, should be zero since the limit is constant but is expressed this way to relate the speed of change to the size of the sideslip error.

## 5.2 Control switch

During driving with a low sideslip angle the agility enhancer will be active. The enhancer will increase the agility of the car and thus the sideslip angle. As the sideslip angle crosses the limit the controller will switch from the enhancer to the sideslip limiter.

To prevent chattering, a transition to smooth out the switch discontinuity is necessary. This can be implemented in the sliding mode control by introducing a boundary layer around the sliding surface. But since the sliding mode controller only will be activated on one side of the surface in the state space, the transition between the signals was implemented outside the sliding mode controller. The transition width between the controllers is set to one degree in the sideslip angle, half a degree below the limit to half a degree above.

## 5.3 Simulation results

The complete controller is a combination of the agility enhancer, the sideslip limiter, the reference generator and the switch. A block diagram, complete with the car and the driver is shown in Figure 14 above.

The effect of the agility enhancer is shown in Figure 15. The figure shows the impact of the feedforward signal on the yaw rate during steady state turning. The effect has been tested on steering angles between 40 and 75 degrees. For steering angels lower than 40 degrees, the agility enhancer is deactivated. For steering angles over 75 degrees, the speed of the car needs to be lower than in these tests.

For low speeds the wheel slips are negligible and the movement of the car is decided only by its geometry. During these speeds the lateral acceleration will have the opposite sign as compared to the speeds giving the results shown in Figure 15. Since the sign of the roll moment distribution depends on the lateral acceleration, the agility enhancer has the opposite effect at lower speeds. Therefore the agility enhancer is deactivated during low speeds.

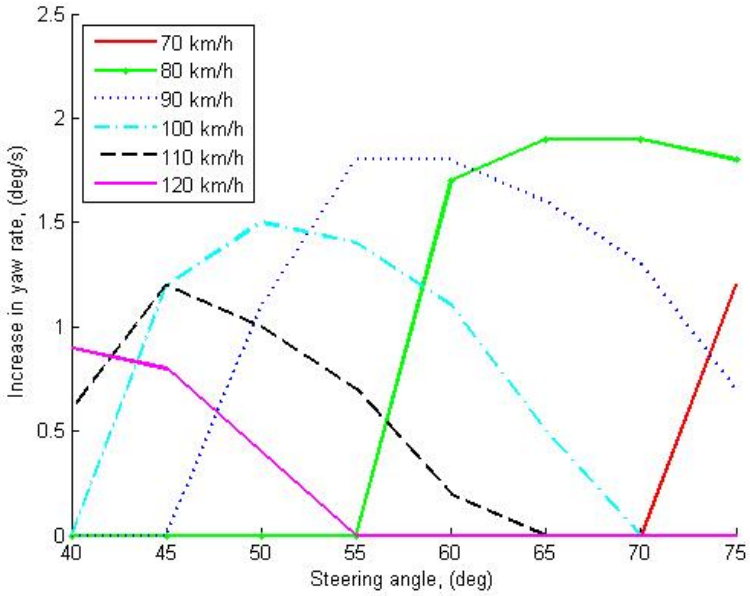


Figure 15. The increase in yaw rate for different car speeds and steering angles in the CASCaDE simulation

For higher speeds in combination with higher steering angles, the yaw rate increase from the agility enhancer will be zero. This is because the car will lose control even without the enhancer. In these situations the enhancer outputs a neutral roll moment distribution and if the car loses control the complete controller changes to the sideslip limiter. Loss of control in this thesis means that the amount of the sideslip angle rapidly grows.

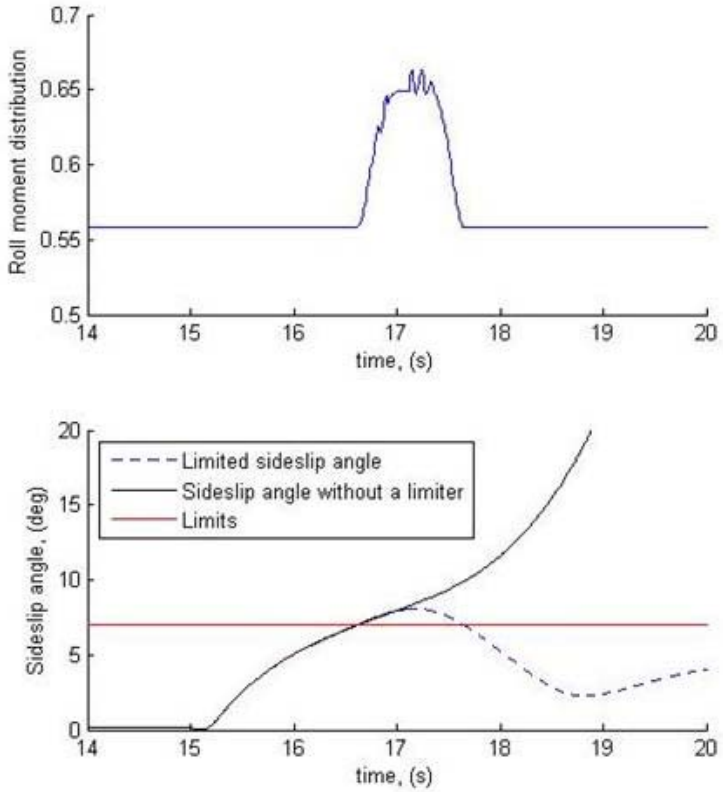


Figure 16. The effect of the sideslip limiter during one turn. Without the limiter the car would lose control entirely. This is a 70 degree turn made at 100 km/h.

Figure 16 above is the result of a simulation showing the impact of the sideslip limiter. The agility enhancer is not active in this simulation, hence, the roll moment distribution is neutral until the sideslip angle crosses its limit. Both the cases with a limiter and without a limiter are shown together with the limit on the sideslip angle in the lower plot.

The roll moment distribution in Figure 16 is rather noisy. As will be explained later, this is an effect of the derivatives of the wheel forces and the noise will be reduced by the actuators of the ABC.

In Figure 17 below the result of the sideslip limiter is shown. The simulation is made during a steady state turn at 90 km/h with a 70 degree wheel angle. Looking at the control signal, the roll moment distribution, it is possible to see the different parts of the complete controller, the agility enhancer, the switch and the sideslip limiter.

As the sideslip angle is lower than its limit, the controller is in the agility enhancing mode with a constant control signal due to the constant speed and steering angle. Then the switch occurs as the sideslip angle is getting closer to its limit. In this simulation the agility enhancer is weighted with 1.10 to assure that the system turns unstable.

It is obvious that the system enters a limit cycle during the steady state turn. But these simulations are made without any action from the driver. Since the driver would take action a steady state turn would not occur, or at least not continue in a real situation.

However, it might be possible to avoid the limit cycle by expanding the sliding surface with the derivative of the lateral velocity instead of only using the lateral velocity, see Section 4.2. This is discussed further in the discussion and future work Section 7.1.

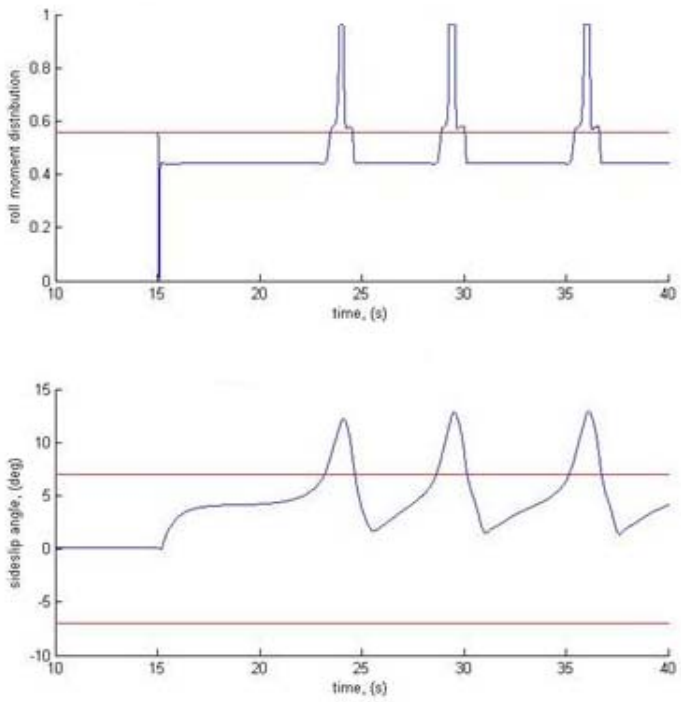


Figure 17. The roll moment distribution (top) and sideslip angle (bottom) during steady state turning. The turn is made at 90 km/h with a 70 degree wheel angle. The straight lines shows neutral roll moment distribution (top) and the sideslip limits (bottom).

Figure 18 below shows a simulation of sinusoidal turning at 110 km/h with a steering amplitude of 70 degrees. The limit of the sideslip angle is set to 4 degrees in this simulation. For higher limits the controller does not manage to limit the slide for this speed and wheel angle. At 90 km/h or 70 km/h it is possible with a higher limit.

When the sideslip limiter is active in Figure 18, the control signal has a noisy character. This noise comes from the part of the controller which considers the derivative of the wheel forces. A lowpass filter should handle this noise efficiently but this is not necessary. The actuator itself, the ABC, has a lowpass filtering effect on its input signal, removing the noise.

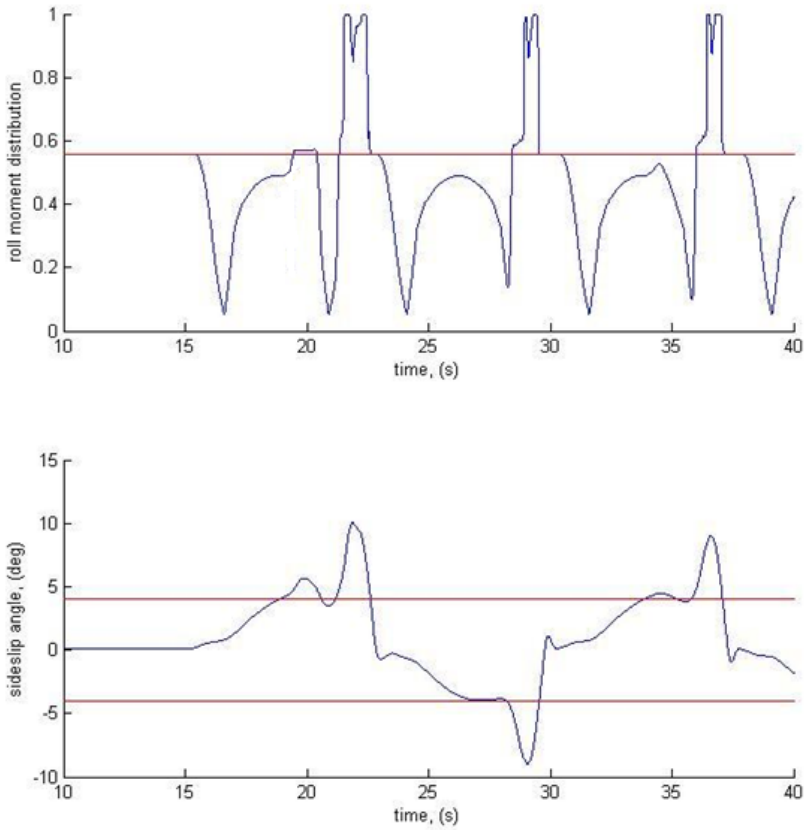


Figure 18. The roll moment distribution (top) and sideslip angle (bottom) during sinusoidal turning. The turn is made at 110 km/h with 70 degree wheel angle amplitude. The straight lines shows neutral roll moment distribution (top) and the sideslip limit (bottom). The limit of the sideslip angle is set to 4 degrees.

For low speeds neither of the two parts of the controller is active. The agility enhancer is only active for speeds over 40 km/h but its effect is negligible for speeds below 60km/h. At high speeds the car loses control too easily, and thus the agility enhancer outputs neutral roll moment distribution.

The sideslip limiter is activated as the velocity of the car reaches ~55 km/h. At these speeds it handles most turns, unless the turning angle is too extreme. At 90 km/h the effect of the limiter is too small to reduce the sideslip unless the limit on the sideslip angle is lowered. In these situations the limiter has the effect of only reducing the rate of loss of control.

## 5.4 Implementation in the car

As discussed above there are two parts in the control signal whose denominator can be zero at times. Most notably the denominator containing the wheel force derivatives. As expected in the discussion above, the wheel force derivatives are much noisier when measured from the car, making the absolute value and limiting necessary.

ESP, or Electronic Stability Control, is a safety measure installed in most cars. It detects loss of steering control and assists the driver in steering the car. It uses the wheels individual brakes to increase or decrease oversteering. The sideslip limiter is designed to take action before the ESP kicks in and should not be active at the same time. Therefore a flag was made indicating when the ESP is active. This flag is constructed by looking at the action on the individual wheel brakes and the steering angle and comparing this with the input from the driver. When the ESP is activated the controller quickly fades out.

Since most of the inputs needed by the sideslip limiter are not measurable, they need to be observed. In [5] an observer of these states is presented. It is an observer developed at Daimler. The inputs to the controller that need an observer are the lateral and longitudinal velocity and the yaw rate. The observation of the wheel forces and the wheel force derivatives are also implemented in the observer.

During the tests the controllers, the reference generator and the switch were implemented in the Simulink environment. The computer running the controllers was connected to the cars CAN-bus via hardware from dSPACE. The ABC is implemented in the test vehicles used.

## 5.5 Test Results

During tests of the controller, the reference generator and the switch has been working as expected. In first tests the ESP kicked in and disrupted the sideslip limiter. This was expected but the range within the controller could work was very narrow. Therefore the remaining test was done with the ESP deactivated. The flag from the ESP and the fadeout when the ESP kicked in was also working correctly.

The test showed that the agility enhancer was working correctly although not to which extent. Further testing of the enhancer will be needed to conclude the effectiveness of the controller on the yaw rate.

The test in the real car was not comprehensive enough to make any conclusions about the effectiveness of the sideslip limiter. Steady state turning is not possible to achieve as easily as in a simulations. However it was evident that the controller will need further tuning and testing to successfully limit the sideslip angle in a car.

# 6. Estimation of longitudinal tyre stiffness

The goal of this estimator is to decide whether the car has winter or summer tyres. If this is known, it can be used to choose the right parameter set for the tyres. This would be very beneficial since an observer of tyre forces, sideslip angle and many other variables could be greatly improved with more precise parameters. At the moment the same set of parameters are used for all tyres.

The longitudinal tyre stiffness, C, is a unitless tyre parameter relating the road-tyre friction, μ, to the longitudinal slip, λ. The road-tyre friction is the ratio between the longitudinal forces, $F_x$, and the wheel loads, $F_z$. The slip is a measurement of the grip of the tyre.

$$\frac{F_x}{F_z} = C \cdot \lambda$$

This relation is only valid during driving with low values on the slip. For more extreme driving the tyres behave nonlinearly.

The longitudinal tyre stiffness differs between summer and winter tyres according to Figure 19 below. The stiffness is significantly higher for summer tyres. According to tyre analysis made by Daimler the summer tyres has a longitudinal tyre stiffness ranging from 30 to 60 units while the stiffness from winter tyres are ranging from 15 to 30 units.

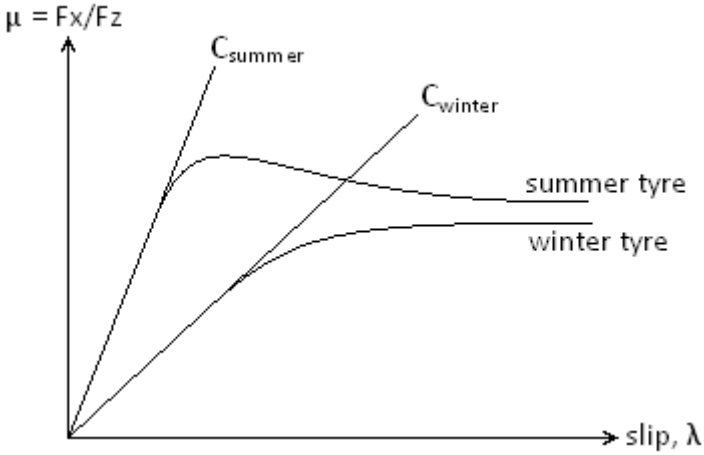


Figure 19. The longitudinal difference between summer and winter tyres

According to the Daimler data, the longitudinal stiffness changes with the wheel load of the car. For a summer tyre the stiffness most often varies with about 6 units from loads changing from 4000N to 8000N on a single wheel, although the variation can be as much as 24 units for some summer tyres. For winter tyres, the stiffness variation is normally up to 5 units with a maximum change at 10 units for the same loads.

With variations up to 5 units it should still be possible to decide which tyre is used with an estimate, but for larger variations, the difference might not be large enough. There are also some questions concerning the data since they do not correspond with various reports such as [11] and [12].

## 6.1 Least squares estimation

Least squares estimation is a way to estimate coefficients from a linear system. A more thorough discussion is found in [9]. A function, f, is wanted which relates a set of measured variables, regressors, to an output

$$y(t) = f(\varphi(t))$$

where

$$\varphi(t) = \begin{bmatrix} \varphi_1(t) \\ \varphi_2(t) \\ \vdots \\ \varphi_d(t) \end{bmatrix}$$

denotes the regressors and $y(t)$ the output at time t. If the function, f, is linear, the relation becomes

$$y(t) = \theta_1\varphi_1(t) + \theta_2\varphi_2(t) + \ldots + \theta_N\varphi_N(t) = \varphi^T\theta$$

where

$$\theta = \begin{bmatrix} \theta_1 \\ \theta_2 \\ \vdots \\ \theta_N \end{bmatrix}$$

are the parameters to be estimated. If data has been collected at several samples at times t = 1 … N, the best estimate of $\theta$, $\hat{\theta}$, is the estimate that minimizes the cost function

$$V(\hat{\theta}) = \frac{1}{2}\sum_{t=1}^{N}\left[y(i) - \varphi^T(i)\hat{\theta}_i\right]^2$$

With the $N \times 1$ vector

$$Y_N = \begin{bmatrix} y(1) \\ \vdots \\ y(N) \end{bmatrix}$$

and the $N \times d$ matrix

$$\Phi_N = \begin{bmatrix} \varphi^T(1) \\ \vdots \\ \varphi^T(N) \end{bmatrix}$$

the minimization criterion can be written in matrix form as

$$V(\hat{\theta}) = \frac{1}{2}\left|Y_N - \Phi_N\hat{\theta}\right|^2$$

This expression is minimized by the estimate

$$\hat{\theta}_N = \left[\Phi_N^T\Phi_N\right]^{-1}\Phi_N^T Y_N$$

which is the least squares estimate of $\theta$.

### Recursive least squares estimation

When used as an online estimator, the least squares algorithm is rewritten as a recursive algorithm to save both calculation time and the number of stored data points. This recursive algorithm also makes it possible to estimate time varying systems by introducing an exponential forgetting factor. The recursive algorithm can be written as

$$\hat{\theta}(n) = \hat{\theta}(n-1) + k(n)\varepsilon(n)$$

$$\varepsilon(n) = y(n) - \Phi^T(n)\hat{\theta}(n-1)$$

$$k(n) = \frac{\frac{1}{\lambda}P(n-1)\Phi(n)}{1 + \frac{1}{\lambda}\Phi^T(n)P(n-1)\Phi(n)}$$

$$P(n) = \frac{1}{\lambda}P(n-1) - \frac{1}{\lambda}k(n)\Phi^T(n)P(n-1)$$

In this algorithm $\hat{\theta}(n)$ denotes the estimate, $\varepsilon(n)$ the error of the estimate and $P(n)$ is the covariance matrix at sample n. The forgetting factor, $0 \leq \lambda \leq 1$, introduces forgetting in the estimator, a smaller value of $\lambda$ reduces the contribution of previous measurements on the estimate. The backside of this is that a smaller $\lambda$ also will increase the estimators' sensitivity to disturbances and because of this $\lambda$ is usually chosen as $0.95 \leq \lambda \leq 1$. When $\lambda = 1$ the estimator has no forgetting at all, turning the estimate into a mean value over time. The number of measurements used in the estimate at time t can be approximated as.

$$N = \frac{1}{1-\lambda}$$

For the recursive least squares, initial values for the estimate and the covariance matrix must be given. With some knowledge of the system, it is possible to give an initial value on the estimate that is of the same magnitude as the actual value. For the covariance matrix, the starting value can be chosen depending on the certainty of the initial guess. Since higher values in the covariance matrix gives larger changes in the initial samples of the estimate, a less certain initial guess of the estimate should be accompanied by a higher covariance.

## 6.2 Modelling

As mentioned above, the longitudinal tyre stiffness relates the longitudinal slip to the road-tyre friction. This relation becomes nonlinear for higher slips. But since the least squares estimator requires linear behaviour, a simplified model will be used. Therefore the model will only be valid for low slip values.

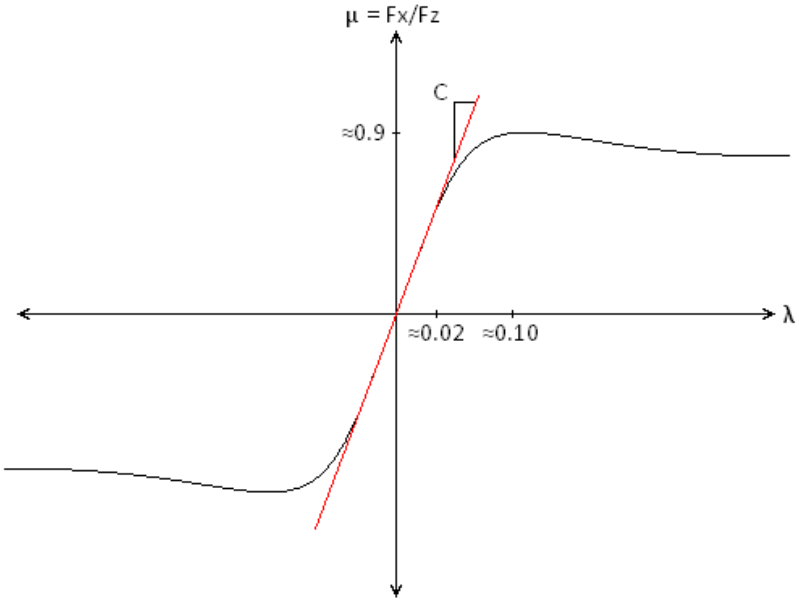

Figure 20. The tyre friction as a function of the longitudinal slip

In Figure 20 above the nonlinear tyre model is approximated by a linear model in the range $-0.02 \leq \lambda \leq 0.02$. As long as the slip is within this range the tyres behave linearly and a least squares estimate is possible. In this range the function can be described by

$$\frac{F_x}{F_z} = C \cdot \lambda$$

Where $F_x$ is the longitudinal force, $F_z$ is the wheel load, $\lambda$ is the longitudinal slip and C is the longitudinal tyre stiffness. The quota

$$\frac{F_x}{F_z} = \mu$$

is known as the road-tyre friction [10]. By choosing

$$y = \frac{F_x}{F_z}, \qquad \varphi = \lambda \quad \text{and} \quad \theta = C$$

the relation can be written as

$$y(t) = \varphi^T \theta$$

This is the form required for the least squares estimator. To be able to use this relation, expressions for the forces and the slip are needed.

### The slip

Accelerating and braking forces in the wheel contact surface are a result of the difference between the wheels circumferential speed and the speed of its CoG. The slip is defined as the difference between the two speeds and is given in percents of the reference speed. $\lambda = 0$ means that the wheel is free rolling with full grip and $\lambda = 1$ that it is spinning without grip.

Since the reference speed of a car is not measurable without GPS, it is here calculated from the front wheels. This is possible since the car can be assumed to be back wheel driven and the front wheels are assumed to roll freely. The reference speed is calculated as a transformation of the front wheel speeds including a component from the yaw rate. This reference speed is then compared

to a mean of the back wheel speeds to get a slip. The following expressions are used:

$$\lambda = \begin{cases} \dfrac{v_r - v_{ref}}{v_{ref}}, & |v_{ref}| > |v_r|, \quad \text{Accelerating slip} \\ \dfrac{v_r - v_{ref}}{v_r}, & |v_r| \geq |v_{ref}|, \quad \text{Braking slip} \end{cases}$$

Where

$$v_r = \frac{1}{2}(v_3 + v_4) \quad , \quad v_{ref} = \frac{1}{2}(v_1 + v_2) - 2 \cdot l_v \cdot \sin(\delta) \cdot \dot{\Psi}$$

The wheel speeds, $v_1$, $v_2$, $v_3$ and $v_4$, cannot be measured directly. Therefore it is necessary to estimate them from the wheels angular speeds. This introduces a new problem for the estimator. The tyre radius is needed and because of tyre deflection, the tyre radius is replaced by the dynamic radius. The dynamic wheel radius was explained earlier in Chapter 2.2.

The main problem for the estimator is, as mentioned above, to decide whether the car has winter or summer tyres, which in turn means that the tyres, and the size of the tyres, will change over time. In addition to this, the tyre deflection depends on the tyre pressure and the wheel load. This means that the dynamic radius will change over time. The impact of these changes will be investigated later in this section. Initially the estimates will be made on equally sized tyres with the same load and the impact of the tyre pressure is assumed to be low.

### The wheel load

The wheel load, $F_z$, is partly measurable in the car. The sensors are positioned in the car suspension and can therefore not measure the load of the wheels and a part of the suspension, the so called unsprung mass. This part of the wheel load is therefore estimated and added to the sensor output.

Another measurement error that needs to be considered is the angle of the suspension. As a car breaks or accelerates the forces influences the pitch of the car, increasing it during a positive acceleration and decreasing it during a negative. To reduce this effect the suspensions are tilted outwards from the centre of gravity. Due to this angle the measurement of the wheel loads also measures a part of the accelerating/breaking force. The same effect occurs when turning since the lateral acceleration affects the roll angle. In this case the suspensions are tilted inwards, changing the measured force depending on the direction of the turn.

The effects during breaking and turning will not be noticed in the estimate since the software will be deactivated during those times. During acceleration the error needs to be reduced. This is done by adding a component to the wheel load proportional to the acceleration.

## The longitudinal wheel force

There are two ways to calculate the longitudinal wheel force, either by using the longitudinal acceleration of the car, or by using the engine torque. Both will be investigated here.

### *The longitudinal wheel force as a function of acceleration*

In Figure 21 below is a force balance of a car driving on a road with inclination θ. There are five different forces acting in the longitudinal direction of the car [10].

- A force from the roll resistance
  $F_{roll} = mgf_r$
  where $f_r$ is the rolling resistance coefficient.

- A part of the gravitational force
  $F_{gravitation} = mg\sin(\theta)$

- A force from the surrounding air.
  $$F_{Aero} = \frac{1}{2}\rho A C_w v_x^2$$
  Here ρ is the density of the air, A is the front area of the car and $C_w$ is the aerodynamic drag coefficient. $v_x$ is the longitudinal velocity.

- A force from the curving resistance
  $$F_{curve} = \frac{m}{2} a_y \delta$$
  where $a_y$ is the lateral acceleration and δ is the steering angle.

- The fifth force is the longitudinal wheel force, $F_x$.

  The force balance becomes:

$$ma = F_x - F_{roll} - F_{gravitation} - F_{Aero} - F_{curve} \Leftrightarrow$$

$$m\left(a_x^s - a_{x0} - g\sin(\theta)\right) = F_x - mgf_r - mg\sin(\theta) - \frac{1}{2}\rho A C_w v_x^2 - \frac{m}{2} a_y \delta$$

The three parts of the acceleration are the sensor output, an offset and a part of the gravitational acceleration from the inclination. This gives the following expression for the longitudinal wheel force

$$F_x = m\left(a_x^s - a_{x0} + gf_r + \frac{1}{2} a_y \delta\right) + \frac{1}{2}\rho A C_w v_x^2$$

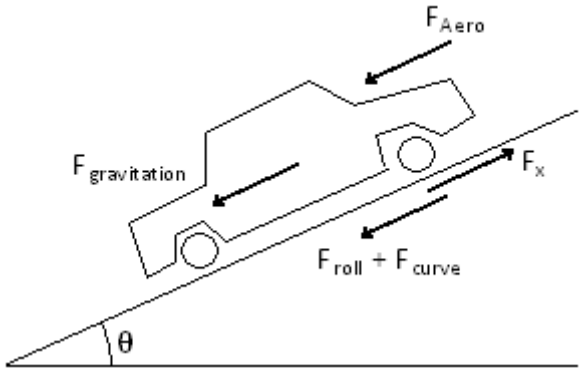

Figure 21. The force balance

*The longitudinal wheel force as a function of engine torque*

Another way of calculating the longitudinal wheel force is by using the engine torque. The torque applied at the wheels from the engine can be calculated as the engine torque, $T_e$, multiplied by the engine to wheel torque ratio, $r_{ew}$. Both the engine torque and the ratio are given.

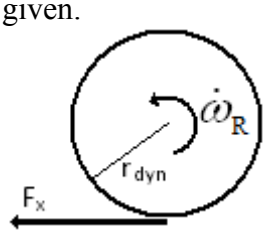

Figure 22. Dynamical radius and angular acceleration

The following torque balance holds for each of the two rear wheels

$$T_e r_{ew} = r_{dyn} F_x - J_\omega \dot{\omega}_R$$

$J_\omega$ is the wheel moment of inertia, $\dot{\omega}_R$ is the angular acceleration and $r_{dyn}$ is the dynamic wheel radius. From this a second expression for the longitudinal wheel force is given.

$$F_x = \frac{1}{r_{dyn}}\left(T_e r_{ew} + J_\omega \dot{\omega}_R\right)$$

## 6.3 Estimation Conditions

Due to the simplifications made in deriving the model, it will not always be valid. Therefore a set of conditions is needed to decide when the system is in the right range for the model and when the observed parameters are correct.

As mentioned above, the linear tyre model is only valid for small values of the slip. The nonlinear range of the tyres begins around $\lambda = 0.02$ making it a good limit for the slip. Lower values on the slip also give inconsistent values in the estimate which results in the following condition on the slip $0.001 \leq \lambda \leq 0.02$

For the calculation of the slip, an assumption that the front wheels are rolling freely was made. Since the estimator only is used for rear wheel driven cars, this is valid as long as the car is not braking. Therefore a condition which requires the braking pressure to be zero, $P_B = 0$, is used. Another reason for using

this requirement is that the observation of the engine torque will not show a breaking torque, it will always be positive.

The estimator is also turned off when the gears are changed. This is because the observer for the engine torque and the engine-wheel torque ratio is sensitive to gear changes. This constraint is not enforced in the estimator based on the acceleration.

In the slip calculation a division is made by the larger one of the reference speed or the rear wheel speed. This makes it necessary to have a constraint on the speed: $v_{ref} > 4$ m/s.

The last requirement on the system is that the car should not be turning. This is because of the simplifications made in the car model earlier. The error becomes more severe at larger accelerations which is why the constraint is enforced on the lateral acceleration instead of the wheel angles: $|a_y| < 0.5$. The effects of these constraints will be discussed later in this section.

## 6.4 Implementation

### Comparison of longitudinal wheel forces

Earlier, two suggestions were given on how the longitudinal wheel force can be calculated. The first one is based on a force equilibrium over the whole car and the second is derived from a torque equilibrium over a single wheel. In Figure 23 below the two forces are plotted.

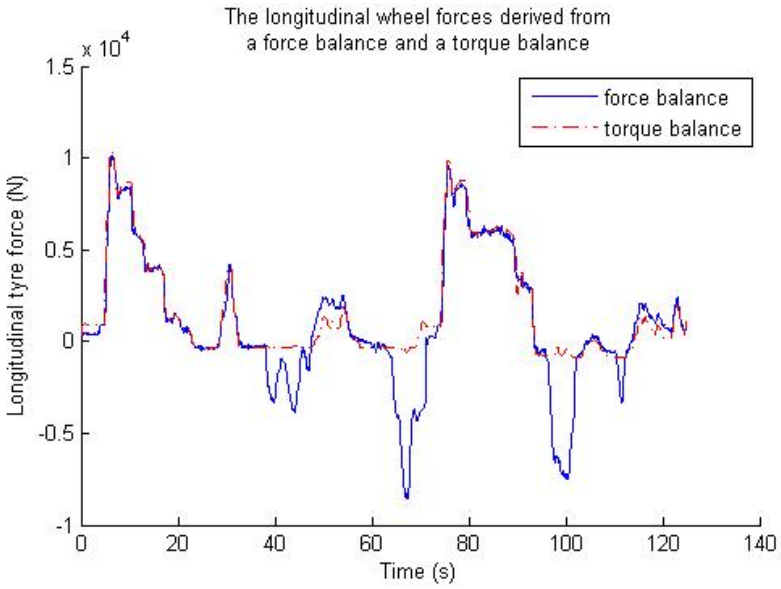


Figure 23. The two different longitudinal tyre forces

The largest difference between the forces is that the one based on the engine torque is always positive. The only time the longitudinal wheel force is negative is when the car is braking and therefore this difference is handled by the requirements on the estimator defined earlier. The other noticeable difference that can be seen in Figure 23 is the peak at 50 seconds. This peak is from accelerating while cornering and will also be handled by the constraints. The same thing happens at 120 s.

A comparison between the estimates using the different longitudinal wheel forces with the constraints active, suggests that both methods are valid. The estimates are very similar with the result based on the engine torque being slightly higher. This can be seen in Figure 24 below.

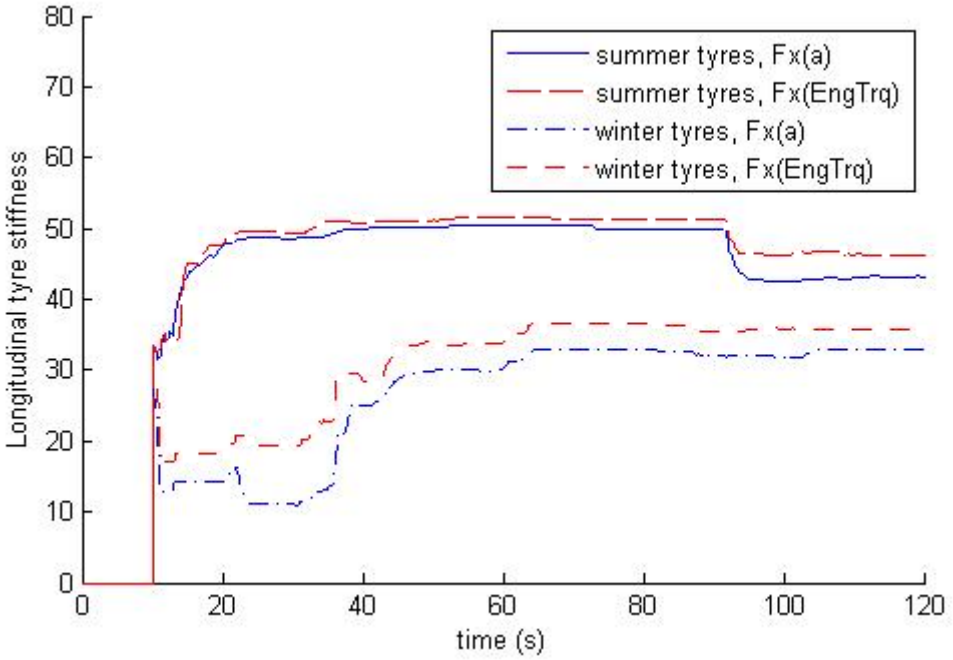


Figure 24. Comparison of the estimates of longitudinal tyre stiffness from acceleration and engine torque.

In Figure 24 the average difference, after convergence, between the summer and winter tyre is 32 % for the estimate based on acceleration and 28 % for the estimate from engine torque. The average difference over several measurements is 24 % for the estimates with acceleration and 18 % for the ones from the engine torque.

From this the conclusion is drawn that an estimate using the slip and a longitudinal wheel forces based on the acceleration fits the purpose of this estimator better than one using a force based on engine torque.

### Effect of the requirements

The requirements for the estimator to be active, defined earlier in this section, improve the estimates substantially. Instead of having the estimator running the whole time, it is now turned off when it is known that the model does not describe the situation sufficiently, or when the inputs to the estimator are expected to be bad.

The used constraints are conservative leading to much of the measured data not being used. The backside of this is that it can take a long time before the estimate converges. During slow, easy driving, the estimator might not be active at all.

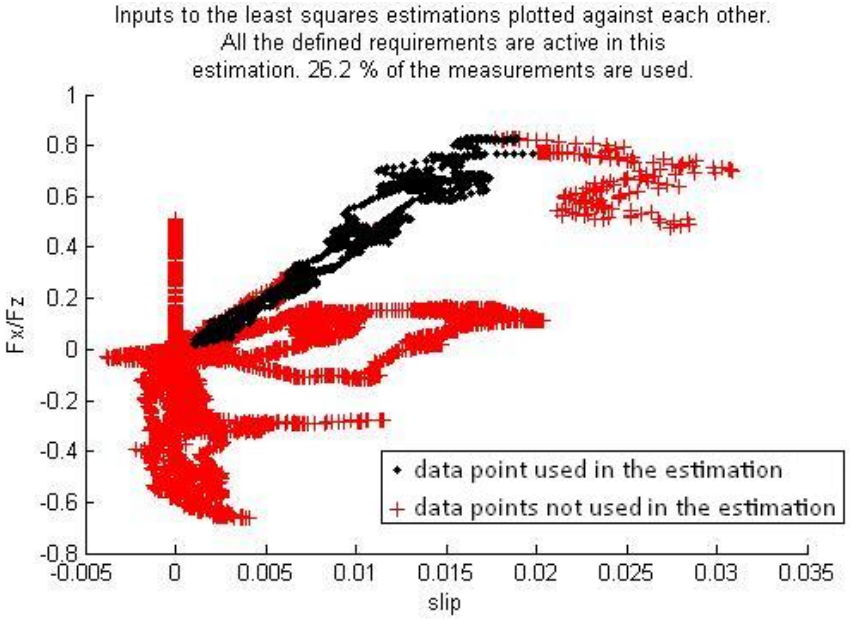


Figure 25. Data points used in the estimate

In Figure 25, the inputs to the least squares estimator are plotted against each other. There it can be seen how conservative the constraints are. The points with $\mu = \frac{F_x}{F_z} \leq 0$ are mostly from braking and the points looping out from the linear region are from turning. The straight line at $\lambda = 0$ are measurements taken at low speeds, $v_x \leq 1$. During these speeds the slip is set to zero to avoid a division by zero.

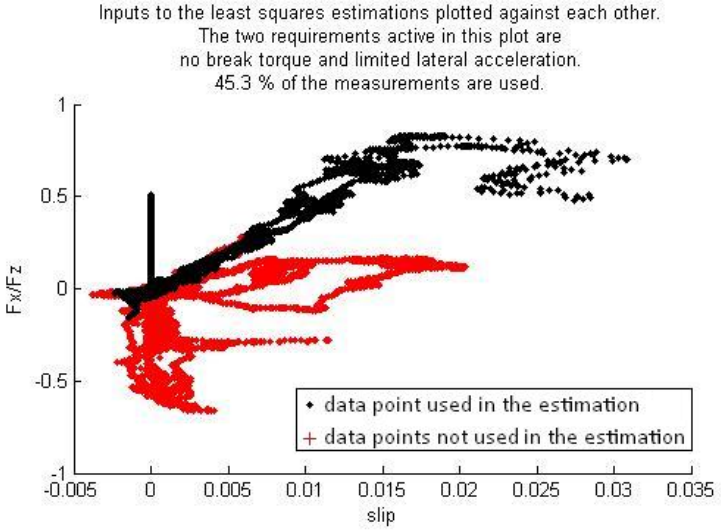


Figure 26. Data points used in the estimate with requirements on the break torque and lateral acceleration are active.

Especially important are the constraints on break torque and lateral acceleration. They have a large influence on the estimate since they disable the estimator when simplifications made are not valid. A plot of the inputs against each other with these two constraints active can be seen in Figure 26.

A plot over the estimated stiffness with three different sets of requirements can be seen in Figure 26. The sets are the two just mentioned above and an estimate without requirements.

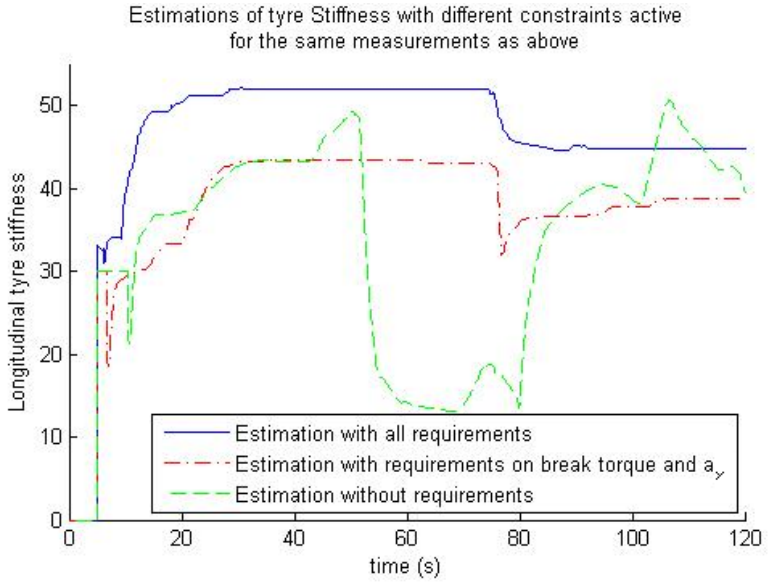


Figure 27. Estimated stiffness with different requirements used

In Figure 27 there is a dip in the two estimates with requirements active after 80 seconds. This is during acceleration after breaking and turning. The estimate with constraints only on break torque and lateral acceleration had a bigger dip here which is explained by a slip that is too high.

### Forgetting factor

The forgetting factor, λ, is used to implement forgetting in the estimator, as mentioned above. The effect of the forgetting factor can be seen in Figure 28. With a value of 0.999 on the factor the estimate becomes much more stable. 0.999 means that roughly the latest 1000 samples are used in each point. With the sample time used in the car 1000 samples is equal to 5 seconds.

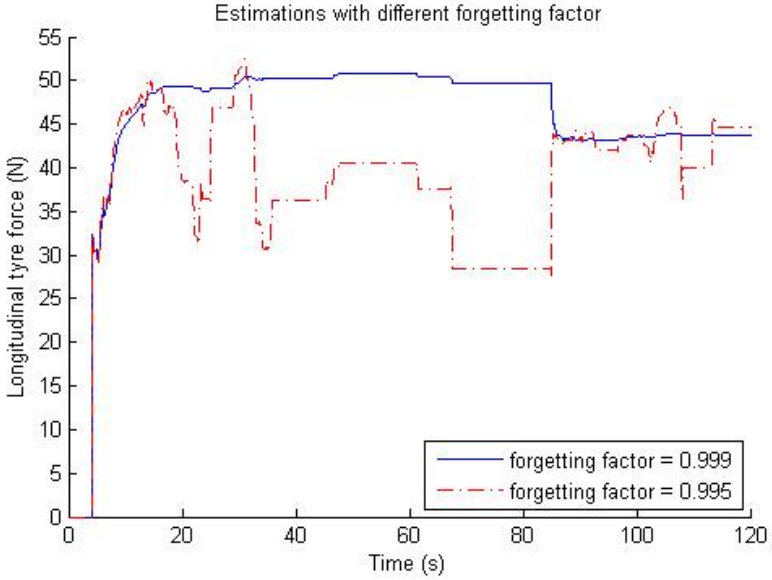


Figure 28. Difference between forgetting factors.

## 6.5 Error sensitivity

To know if the difference in the estimates of summer and winter tyres is enough, estimates of the possible errors are needed. In this part the effect of errors on the several different inputs will be investigated.

Least squares smoothes noise disturbances on the inputs since it calculates the mean over time of the relation between the inputs. Therefore noise disturbances do not have an impact on the result. But with the constraints on the estimation defined earlier this might change. For example if the slip is close to its lower limit and has a larger noise disturbance, the noise might push the signal under its limit. The estimator will then be deactivated when the slip is too low and the mean of the used slip will be slightly higher than the actual slip.

### Slip and Tyre friction

Since least squares is a linear method, load disturbances on its inputs will propagate linearly. A 5% positive error on the slip gives rise to a 4.5% negative error in the estimate. Similarly a 5% positive error in $\mu$ will propagate to a 4.9% positive error in the estimate.

For a disturbance in the form of white noise, a standard deviation of 5% will result in a stable error of 4.5% for the slip. This is for a situation with a low slip, for higher slips the effect is negligible. The reason for this difference is explained above in the introduction to this Section 6.5. Noise has a very small impact on the road-tyre friction.

### Wheel speeds

Disturbances on the wheel speeds have a large effect on the slip while the tyre friction is unaffected. A 10% load disturbance on one wheel propagates to an offset in the slip of 0.005. If this disturbance is affecting the front wheels, the offset will be negative and turn the slip negative for a large part of the measurement. This will deactivate the estimator due to the constraints enforced earlier. If the disturbance affects both front and back wheels the effect will be cancelled out.

The sensor of the wheel angular speed is essentially a cog wheel where a magnetic sensor registers the edges of each cog. This introduces a delay at lower speeds but, as mentioned above, this will not affect the estimate. Another source of errors is that dirt and wearing of the cogs can manipulate the readings of the sensor, but this is handled by logics in the measurement software.

This sensor outputs the angular speed of the wheels and not the circumferential speed that is needed for the estimator. As explained above, this introduces a problem with the dynamic wheel radius, $r_{dyn}$.

### Dynamic wheel radius, $r_{dyn}$

For an 18 inch tyre, a one inch difference between the nominal value and the real value is 5.6%. For the error propagation, a 10% error in the dynamic wheel radius will give a 0.6 % error in the estimate.

However a more serious problem might occur. It is possible that the front wheels are of a different size than the back wheels. With a nominal value on $r_{dyn}$ this will give a large error in the slip. A one percent error on $r_{dyn}$ for either the front or back wheels will result in an error for the estimate of about 4 %. The issue

with this is that if the front wheels are smaller than the dynamic radius, the slip might become negative. This would deactivate the estimator.

### Wheel loads

A disturbance in the wheel loads, $F_{zi}$, will only be noticed in the calculation of the tyre friction, $\mu = \frac{F_x}{F_z}$, the disturbance will propagate linearly and a 5% load disturbance will result in a ≈5% error in μ and, later, in the estimate.

One error source in this signal is the estimated unsprung mass. This estimated mass is about 20 kg per wheel making it ≈3.5% of the entire wheel load. An error on this mass would only be very small percentage of the total load.

As mentioned above in the modelling, the wheel load sensors are affected by turning and positive as well as negative accelerations, although these effects only need to be considered during positive accelerations. The effect is reduced by adding a component to the loads, proportional to the acceleration. With this correction the worst case error is estimated to ≈2%.

### Longitudinal acceleration

The longitudinal acceleration is a substantial part of the calculation of the longitudinal tyre force. It is also an important quantity to the estimator requirements since the software is only active during accelerations.

In the car used for taking measurements there are three different sensors for the lateral acceleration. The alignment of two of those is not known and this might add an unknown component to the measurement. The third sensor does not have a tilt component since it is known to be correctly aligned. The difference in the estimations from these three acceleration signals is not larger than 3 %.

### Mass

As the mass changes, so does the behaviour of the car. The impact of this can be seen in Figure 29 below. The mass increase is 200 kg, 8%, and this result in a 5.8% decrease in the estimate. The difference vanishes if an appropriate change in the nominal mass is made, but since the mass is unknown during a real estimation this cannot be done.

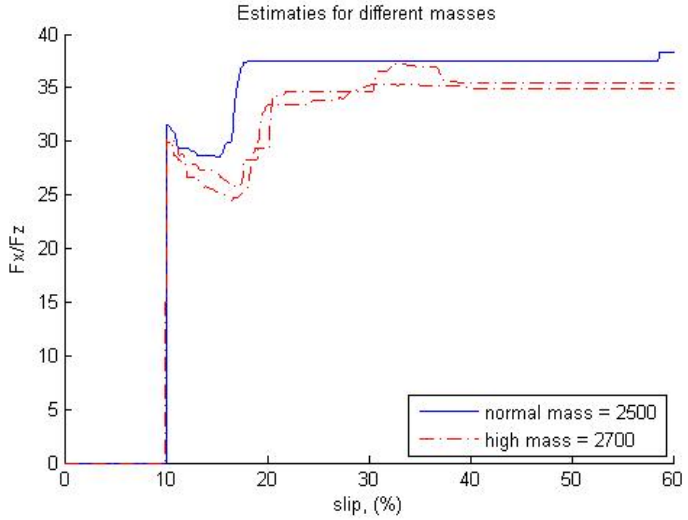


Figure 29. A higher mass gives a lower estimate.

### Road surface

The effect of different road surfaces has been tested to the extent that an estimate from an uneven, bumpy road surface is compared to one from a normal road surface. These tests implies that the effect of the road surface is small.

The estimator has not been tested on other surfaces such as wet or icy roads, but according to [11], these different conditions influence the estimate in a considerable way.

### Tyre pressure

Since the tyre pressure has an effect on the dynamic wheel radius it will also affect the estimate. According to the plot below, Figure 30, an increase of 11% in the tyre pressure results in a ≈ 12% decrease in the estimated stiffness. This is probably mostly due to the change in the dynamic wheel radius as mentioned above, and will probably be greatly reduced with an on-line estimate of the radius.

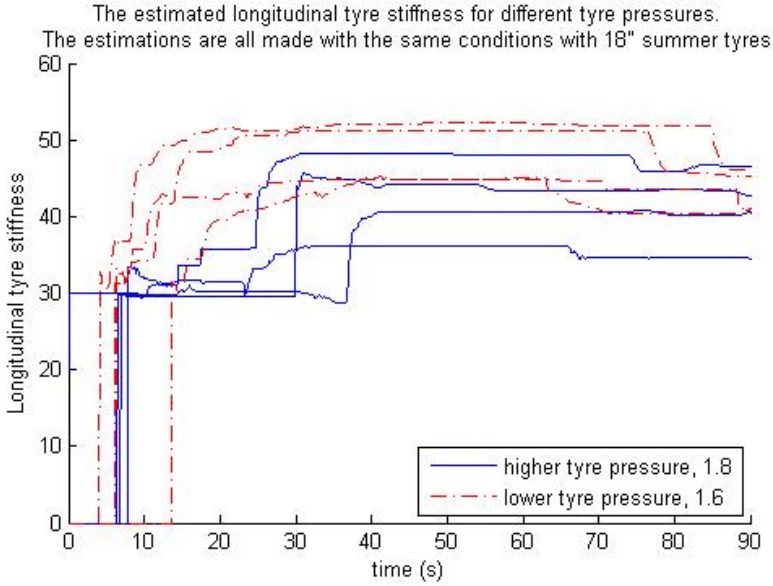


Figure 30. Different tyre pressures

### Summary

The mass and dynamic wheel radius are expected to be the largest error sources. Tyre pressure is also expected to have a substantial impact but this is most likely coupled with the dynamic wheel radius

The wheel speeds might also have a noticeable impact during times when the slip is close to its limits, but this should only deactivate the estimator and not change the result and an error on this signal is unlikely. A larger error on the wheel loads or the longitudinal acceleration is also unlikely.

## 6.6 Test results

In Figure 31 below four different estimates are shown, two of each type of tyre. The difference in longitudinal tyre stiffness between the tyres is 10 – 11 units, making it a ≈20% difference. The two summer tyre estimates are both made

during one acceleration while for the two winter tyres the estimates are made during two shorter accelerations. That is why the winter tyres converge slower, the acceleration is lower and lasts a shorter time.

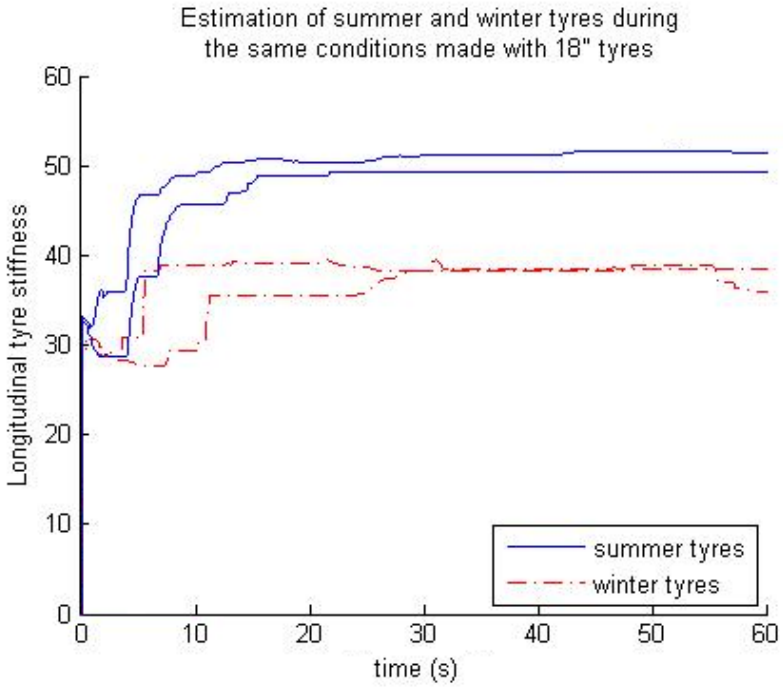


Figure 31. Results of estimates

As mentioned earlier the worst error sources are mass, wheel radius and tyre pressure. The error from the mass in these measurements is a result from the unknown amount of petrol, and the unknown passenger weight. This error is estimated to be in worst case 5% on the estimation.

The error in the dynamic wheel radius is believed to be less than 5 %. This is because the tyre size is known, and that it is known that all tyres have the same size. This error propagates to about 2% in the estimation.

Another error with a significant impact is the tyre pressure. It is hard to see the impact of this since is it coupled with the dynamic wheel radius but the error is expected to be 5% of the pressure in worst case. This means an error of ≈ 5% on the estimate.

The remaining error sources are expected to give rise to a collected error of 3-4% in worst case. The resulting error in the estimate is thus believed to be 15% in a worst case scenario.

This is to be compared to the 20 % difference between the estimates in Figure 31. It should also be considered that these estimates are made during a specific scenario with the same accelerations and it was known that equally sized wheel was used front and back.

The estimator has so far been tested on a couple of different driving situations: the autobahn, roads on the countryside and driving in towns. Due to the season of the year the estimator was made and to German law, it has not been possible to test the estimator on winter tyres for these types of roads. Therefore the following results are all for summer tyres.

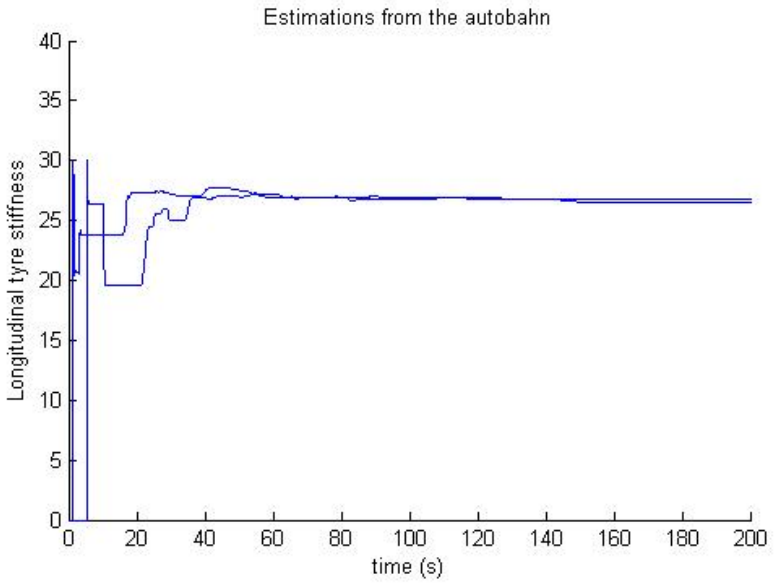

Figure 32. Estimates from the autobahn

In Figure 32 to 34 the three different scenarios are presented. As can be seen the estimates are stable but with a decreasing stability for slower roads, i.e. a road which allows a high acceleration will have estimates which converge faster and less speed changes will result in an estimate with less changes . The frequent changes in the estimates in a town are due to the nature of city driving.

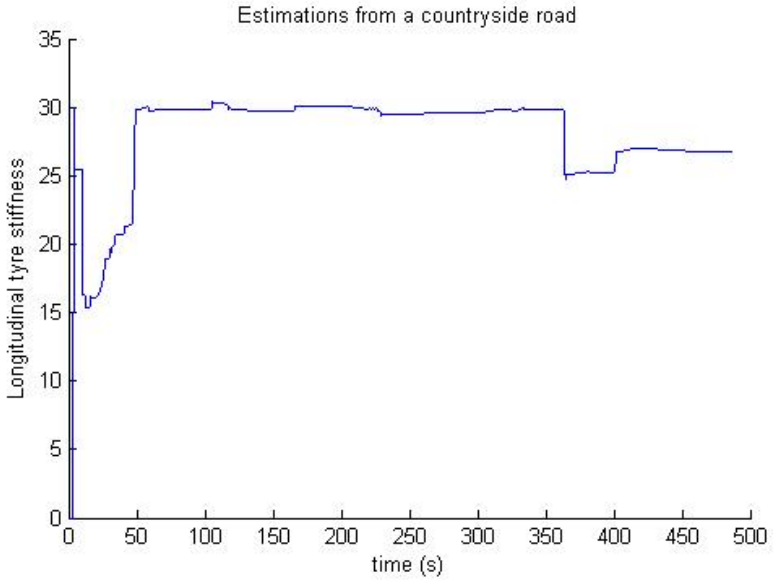

Figure 33. An estimate from driving on a countryside road.

In these measurements it is still known that the wheel sizes are equal for all four wheels and thus it is possible to use a nominal value on the dynamic wheel radius. The estimates where made with a low amount of petrol in the tank giving an error in the nominal mass. For the tyre pressures, they are a little bit higher since the tyres where changed just before these test where made. Because of this, the mass and the tyre pressure, the estimates should be on the low side. But not as low as Figure 32-34 show.

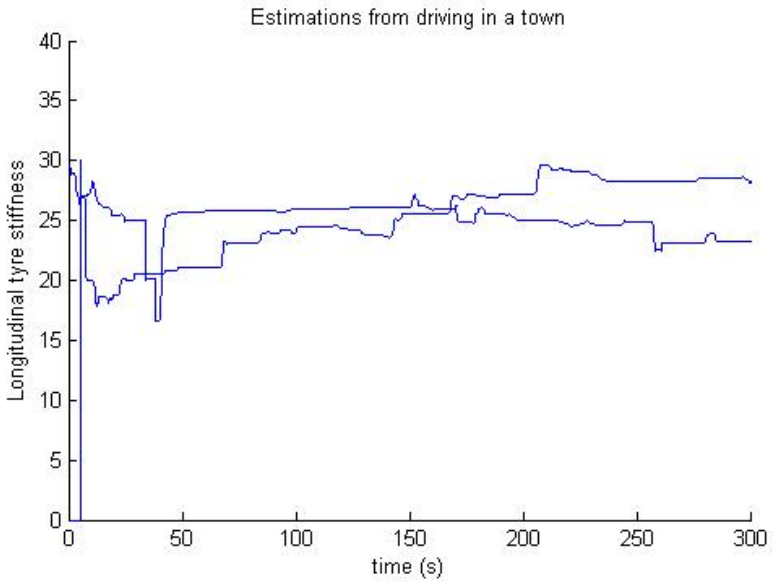

Figure 34. Estimate from driving in a town

A reason for this very low result is that the tyres were brand new. New tyres can be expected to behave differently for about the first 20 km and these tests were made directly after the change of tyres. The different behaviour occurs because of a plastic layer on the tyres that is worn down first after some kilometres. This layer is expected to lower the stiffness which agrees with the results.

# 7. Discussion and future work

## 7.1 The agility enhancer and the sideslip limiter

The agility enhancer is working as expected. It successfully raises the yaw rate during turning although it also affects the sideslip angle. In many cases the sideslip angle is very close to unstable angles. This would be useful if the sideslip limiter wouldn't give rise to the limit cycles that is appearing during steady state turning. The reason for that will be explained later in this section.

The sideslip limiter is successfully limiting the sideslip angle. It works in a rather narrow band from 50 km/h to 90 km/h or up to 110km/h depending on the limit on the sideslip angle. For steady state turning, the system enters a limit cycle where the sideslip angle is oscillating around the limit. This is in combination with the agility enhancer.

Figure 13 in Section 4.2 shows a sinusoidal turn at 120 km/h of 75 degrees. This is possible since the sideslip angle was not growing rapid. The reason for this is that the agility enhancer was deactivated during that simulation.

One reason for the limits cycle can be the simplifications made in the wheel model. A more exact model of the car dynamics might improve the result of the controller.

As mentioned in Section 5, the controller might be improved if more states are included in the derivation of the sliding mode controller. The controller which has been used is based on a sliding surface consisting only of a requirement on the lateral velocity. If a requirement on the time derivative of the lateral velocity also would be included, the controller would be working on the speed of change of the velocity error as well as the actual error.

In Figure 35 the sliding surface which has been used so far is shown. It is described by:

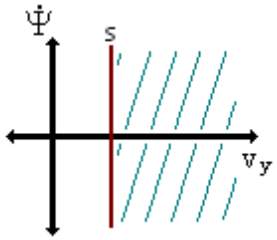

Figure 35. The sliding surface used so far.

$$s = \left(v_y - v_{yD}\right) = 0$$

The new surface would instead be described by:

$$s = \left(v_y - v_{yD}\right) + \lambda \cdot \left(\dot{v}_y - \dot{v}_{yD}\right) = 0$$

With this the new Lyapunov function would become:

$$\dot{V} = s \cdot \dot{s} = \left(v_y - v_{yD}\right) \cdot \left(\dot{v}_y - \dot{v}_{yD}\right) + \left(\dot{v}_y - \dot{v}_{yD}\right) \cdot \left(\ddot{v}_y - \ddot{v}_{yD}\right)$$

The second derivative of the lateral velocity is:

$$\ddot{v}_y = -v_x \ddot{\Psi} + \dot{a}_y .$$

Since the model of the car is derived from Newtons second law, the derivative of the acceleration is not included.

Despite this a small test was made on a version of this new version of the sideslip limiter. This new controller used the new sliding surface but with the former control law defined in Section 4.2. This new sliding surface used the surface described by:

$$s = \left(v_y - v_{yD}\right) + \left(\dot{v}_y - \dot{v}_{yD}\right) = 0$$

Since this surface does not correspond to the control law defined in Section 4.2 a few modifications had to be made to the controller. As mentioned in the theory, a sliding mode controller is a robust controller that can overcome uncertainties as long as the sliding surface is known and used in the control law. This is possible by making the controller less precise but more robust.

In this case, the controller is only used on one side of the surface and deactivated on the other side. This in combination with a higher tuning variable makes it possible to use the controller with the new sliding surface. Figure 36 below shows the result. In the simulation a more aggressive turn is made than in the simulations before, this controller is capable of handling more extreme situations.

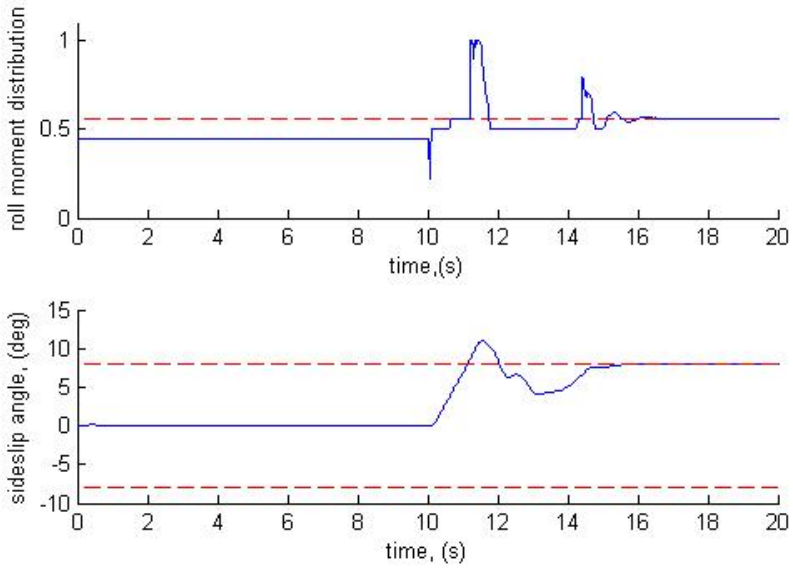


Figure 36. With the controller with a new sliding surface, it is possible to handle more extreme situations. This shows a simulation of a steady state turn of 75 degrees at 120 km/h. The controller gives rise to an over-shoot but no limit cycles. A stronger turn or higher speed will cause a loss of control. The limit of the sideslip angle is 8 degrees.

This sliding mode control in combination with an agility enhancer with a small gain = 1.1 would give the car new characteristics. As the car would start turning, the agility enhancer would force the car to become unstable, activating the sideslip limiter. Since limit cycles would not occur, the two controllers would force the car to have a fixed sideslip angle. The two controllers would track the set sideslip angle. This happens in Figure 36 above.

## 7.2 Estimation of longitudinal tyre stiffness

Generally the estimates of summer tyres correspond well to the values suggested by the summer tyre data from Daimler. This data suggests that the stiffness ranges from 30 to 60 while the estimates mostly range from 40 to 50. For the winter tyres the estimates are on the high side. The data ranges from 15 to 30 while the

estimates range from 25 to 40. However, the data from Daimler should not be completely trusted. According to this data, the tyre pressure does not affect the longitudinal stiffness at all; something which the estimator suggests affects the stiffness linearly. A 1% increase in the tyre pressure gives a 1% higher estimate. Since the data cannot be entirely trusted, the difference between summer and winter tyres is not completely known.

It has been suggested above that the estimator is very sensitive to changes in the mass and in the wheel radius. The result of a mass change still has to be investigated further since the behaviour remains partly unclear. For the wheel radius, the estimation is only sensitive to differences between the radius of the front and the beck wheels.

The wheel radius is only used to calculate the car reference speed and the mean speed of the back wheels. The reference speed can be measured using GPS and with such a signal the dynamic wheel radius can also be calculated. This would eliminate the problem with the radius.

A solution to the two sensitivity problems is to estimate the mass and wheel radius and use the results in this estimator. This however, can be complicated since different relations than the one used here must be found. The estimate of mass would only have to be activated for some time directly after the car starts driving since a change in mass is improbable while $v_x \neq 0$. The wheel radius would only be active directly after the car has been turned off since a wheel change with the car active is equally improbable.

One suggestion is to use the relation between the wheel force and the engine torque described and tested above. This might prove useful to estimate the dynamic wheel radius. Another approach is to use the engine torque and wheel force to estimate the tyre stiffness and use the equation from the force balance to estimate the mass.

Because of the requirements for the estimator to be active, it is possible that it will not be active at all during some scenarios. This is in situations such as city driving and other slow, high steering scenarios. But considering the reason for the estimator this is not a big problem. A good parameter set for the tyres is mostly needed for more extreme driving situations and before this happens it is probable that the estimator has been active.

# 8. Bibliography


[1] Robert Bosch Gmbh
Safety, Comfort and Convenience Systems
Wiley & Blackwell, 2006

[2] Anders Widd
Estimation of Side Wind Disturbances in Automotive Vehicles
Daimler AG, 2006

[3] Peter Clarke
Adaptive cruise control takes to the highway
EE Times, 10/20/1998

[4] Don Sherman
Electronic Chassis Control
Automotive Industries, 1999

[5] Jens Kalkkuhl
Technischer Bericht
Daimler AG, 2009

[6] Magnus Rau
Koordination aktiver Fahrwer-Regelsysteme zur Beeinflussung der Querdynamik mittels Verspannungslenkung
Daimler AG, 2007

[7] Jens Lüdemann
Heterogeneous and hybrid control with application in automotive systems
University of Glasgow, 2002

[8] Jean-Jacques E. Slotine
Applied nonlinear Control
Prentice Hall 1991

[9] K. J. Åström, B. Wittenmark
Adaptive Control, 2nd ed.
Prentice Hall, Eaglewood Cliffs, 2006

[10] Thomas Gillespie
Fundamentals of vehicle dynamics
Society of Automotive Engineers, Inc., 1992

[11] Canudas-de-Wit, Tisotras, Velenis, Basset and Gissinger
Dynamic Friction Models for Road/Tire Longitudinal Interaction
Article in Vehicle System Dynamics,
VOL 39; PART 3, pages 189-226
Swets & Zeitlinger BV, 2002

[12] Burckhardt
Radschlupf-Regelsysteme
Vogel 1993